

AD-A047 144

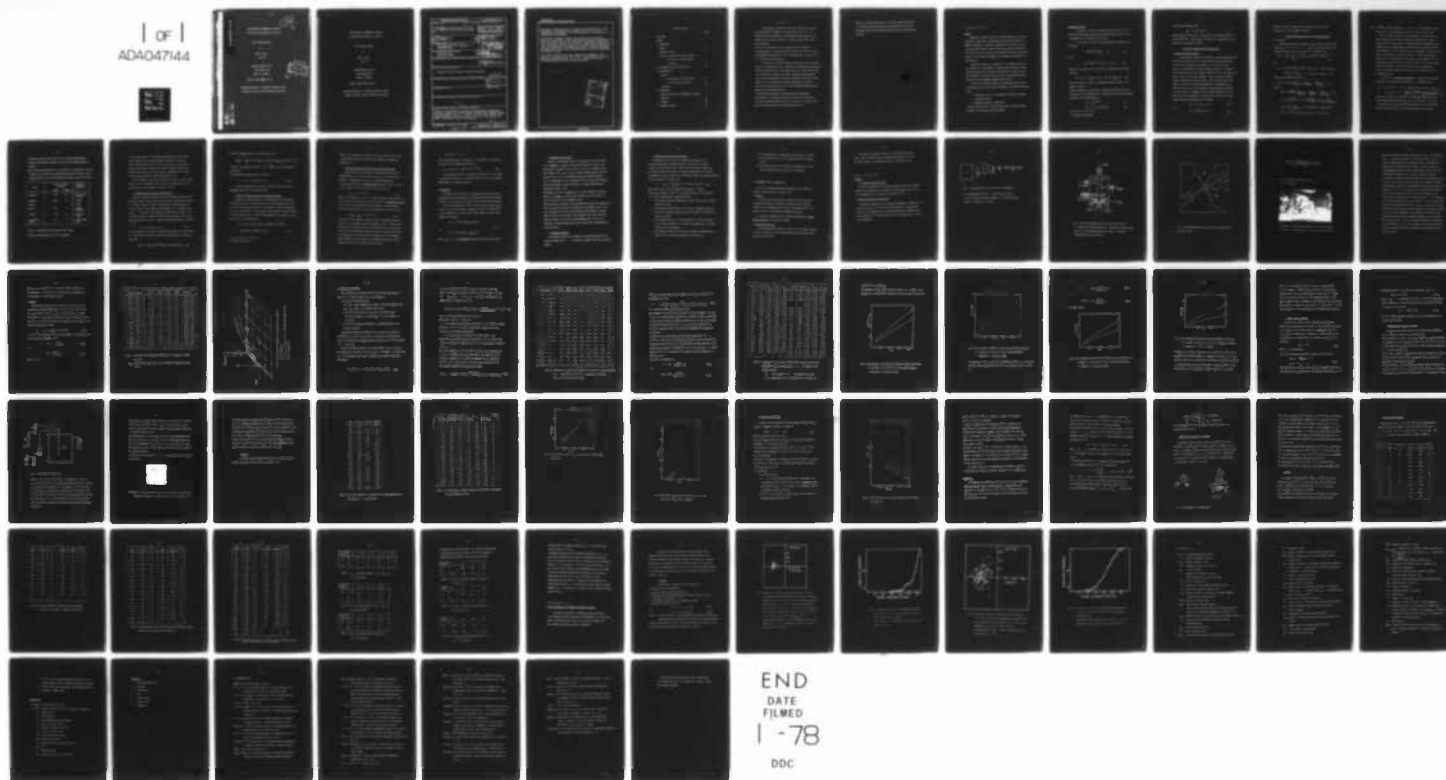
HEBREW UNIV JERUSALEM (ISRAEL)
THE DYNAMICS OF NON SPHERICAL PARTICLES.(U)
JUN 77 I GALLILY

F/G 4/1

DA-ERO-75-G-021
NL

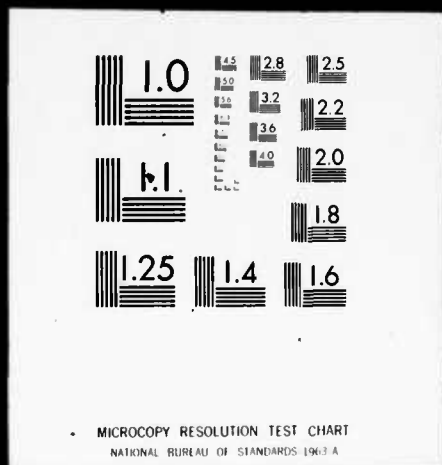
UNCLASSIFIED

1 of 1
ADA047144



| OF |

ADA047144



AD A047144

THE DYNAMICS OF NONSPHERICAL PARTICLES
III. Mobility and Deposition in Still Air

Final Technical Report

by

Isaiah Gallily

June 1977

European Research Office

United States Army

London W.1, England

Contract Number DAERO-75-G-021

The Hebrew University of Jerusalem, Jerusalem, Israel

Approved for public release; distribution unlimited

AD NO. _____
DDC FILE COPY

DDC
RECEIVED
NOV 21 1977
F

THE DYNAMICS OF NONSPHERICAL PARTICLES

III. Mobility and Deposition in Still Air

Final Technical Report

by

Isaiah Gallily

June 1977

European Research Office

United States Army

London W.1, England

Contract Number DAERO-75-G-021

The Hebrew University of Jerusalem, Jerusalem, Israel

Approved for public release; distribution unlimited

REPORT DOCUMENTATION PAGE		READ INSTRUCTIONS BEFORE COMPLETING FORM
1. REPORT NUMBER	2. GOVT ACCESSION NO.	3. RECIPIENT'S CATALOG NUMBER
4. TITLE (and Subtitle) (6) THE DYNAMICS OF NON SPHERICAL PARTICLES		5. TYPE OF REPORT & PERIOD COVERED (7) FINAL TECHNICAL REPORT 1 Mar 75—1 Jun 77
		6. PERFORMING ORG. REPORT NUMBER
7. AUTHOR(s) (10) ISAIAH GALLILY		8. CONTRACT OR GRANT NUMBER(s) (15) DAER8-75-G-021
9. PERFORMING ORGANIZATION NAME AND ADDRESS THE HEBREW UNIVERSITY OF JERUSALEM JERUSALEM, ISRAEL		10. PROGRAM ELEMENT, PROJECT, TASK AREA & WORK UNIT NUMBERS 6.11.02A-2M061102B53B-00- 328 (16) (17) 00
11. CONTROLLING OFFICE NAME AND ADDRESS USA R&S GP (EUR) BOX 65 FPO NY 09510		12. REPORT DATE (11) JUNE 1977
		13. NUMBER OF PAGES 72 (12) 75 p.
14. MONITORING AGENCY NAME & ADDRESS (if different from Controlling Office)		15. SECURITY CLASS. (of this report) UNCLASSIFIED
		15a. DECLASSIFICATION/DOWNGRADING SCHEDULE
16. DISTRIBUTION STATEMENT (of this Report) Approved for Public Release, Distribution Unlimited.		
17. DISTRIBUTION STATEMENT (of the abstract entered in Block 20, if different from Report) <div style="text-align: right;">DDC RECEIVED NOV 21 1977 RESERVED F</div>		
18. SUPPLEMENTARY NOTES		
19. KEY WORDS (Continue on reverse side if necessary and identify by block number)		
<p style="text-align: center;">→ In this paper</p>		
20. ABSTRACT (Continue on reverse side if necessary and identify by block number) In this, his latest report on this topic, the aerodynamic translational mobility of nonsphericals was experimentally determined by Professor Gallily for Knudsen numbers of up to 0.2. The particles were glass cylinders, which represent asbestos fibers and ice needles, and cubes, which represent the primary constituents of metal oxide aggregates. → next page PTO		

165450

UNCLASSIFIED

SECURITY CLASSIFICATION OF THIS PAGE (When Data Entered)

→ The method of determination and the apparatus used were based on a stereo-photography of the trajectories of the particles in still air and a photogrammetric measurement of the (three) dimensions of the particles in a scanning electron microscope.

The results for cylinders, compared with continuous fluid theoretical values of the coefficients, show a reasonable correspondence with expectation which even improved when the blunt edge effect of the particles was taken into consideration. However, in the case of cylinders having diameters above 1 μm , the experimentally determined coefficients were higher by about 50% than the continuous fluid calculated ones, whereas in the case of cylinders of diameters less than 0.5 μm , the determined coefficients were smaller than the calculated values.

The resistance coefficients of cubes showed similar tendencies. The deposition of cylindrical particles in still air was studied in a specially constructed sedimentation cell; in this cell, a method for the size distribution analysis of these particles was tried.

micrometers

ACCESSION for	
NTIS	Write Section <input checked="" type="checkbox"/>
DDC	B.H. Section <input type="checkbox"/>
UNANNOUNCED	<input type="checkbox"/>
JUSTIFICATION	<input type="checkbox"/>
BY	
DISTRIBUTION AVAILABILITY CODES	
Dist.	SP. CIAL.
A	

UNCLASSIFIED

TABLE OF CONTENTS

	Page
Title Page	
SUMMARY	
I. INTRODUCTION	
General	1
Equations of motion	2
Scientific background and previous studies	
a. Mobility, Forces, and Torques	3
b. Deposition	10
II. STATEMENT OF AIM OF REPORTED STUDY	13
III. EXPERIMENTAL	
Mobility	
a. Cylindrical Aerosol Particles	14
b. Cubical Aerosol Particles	31
Deposition	41
IV. THEORETICAL	
Spatial distribution of sedimented cylindrical particles	52
V. GLOSSARY	58
VI. LITERATURE CITED	63

S U M M A R Y

The aerodynamic translational mobility of nonspherical particles was experimentally determined for Knudsen numbers of up to 0.2. The particles were glass cylinders, which represent asbestos fibers and ice needles, and cubes, which represent the primary constituents of metal oxide aggregates.

The method of determination and the apparatus used were based on a stereo-photography of the trajectories of the particles in still air and a photogrammetric measurement of the (three) dimensions of the particles in a scanning electron microscope.

The results for cylinders, compared with continuous fluid theoretical values of the coefficients, show a reasonable correspondence with expectation which even improved when the blunt edge effect of the particles was taken into consideration. However, in the case of cylinders having diameters above $1\text{ }\mu\text{m}$, the experimentally determined coefficients were higher by about 50% than the continuous fluid calculated ones, whereas in the case of cylinders of diameters less than $0.5\text{ }\mu\text{m}$, the determined coefficients were smaller than the calculated values.

The resistance coefficients of cubes showed similar tendencies.

The deposition of cylindrical particles in still air was studied in a specially constructed sedimentation cell; in this cell, a method for the size distribution analysis of these particles was tried.

Finally, the spatial distribution of sedimented cylindrical particles on an horizontal plane was theoretically calculated by extending the Monte Carlo method of Gallily and Cohen for treating rotating Brownian particles.

I. INTRODUCTION

General

Deposition of aerosol particles on various obstacles is of extreme importance in many natural, technological, and scientific systems. For example, performance of industrial installations for abatement of particulate pollutants (spray scrubbers, cyclones, electrical precipitators, and fibrous filters), air pollution field samplers (impactors, small-pore filters), and the human lung, depends on the deposition characteristics of the particles.

Analyzing the behaviour of aerosols in the collecting systems, one is confronted with the significant difference between spherical and non-spherical particles. The difference is mainly due to the poor, or even lack of symmetry of the latter (Gallily, 1974), which makes the understanding of their aerodynamic behaviour very difficult.

To achieve a workable knowledge of the aerodynamic behaviour and the deposition rate of the particles on obstacles, one usually follows two lines:

- a. Theoretical solution of the equations of motion for typical, illuminative cases;
- b. Experimental studies of these cases.

Obviously, the lines have to complement each other, thus establishing confidence in the method of problem treatment.

Equations of motion

Depending on the size of the particles and the nature of the flow which carries them, one can deal with the motion of the former from a deterministic or a stochastic point of view.

In the first, one has to solve the equations of translation and rotation.*

$$m \frac{d\vec{u}_m}{dt} = \sum_i \vec{F}_{e,i} + \vec{F}_F \quad [1]$$

and

$$\vec{I}_m \cdot \frac{d\vec{\omega}}{dt} = \sum_i \vec{L}_{m,e,i} + \vec{L}_{m,F} \quad [2]$$

whereas in the second, one has to deal with the equation of convective diffusion

$$\partial c_i / \partial t + (\vec{v} + \vec{B} \cdot \vec{F}_e) \cdot \vec{\nabla} c_i = \text{div} (kT \vec{B} \cdot \vec{\nabla} c_i) \quad [3]$$

which are subjected to initial and boundary conditions typical of the physical situation.

The main difficulty in the solution of equations [1]-[3] lies with the evaluation of the fluiddynamic force, torque, and mobility tensor, formally defined for a continuous medium by

$$\vec{F}_F = \int_S d\vec{S} \cdot \vec{\pi} \quad , \quad [4]$$

$$\vec{L}_{m,F} = \int_S \vec{r}_m \times (d\vec{S} \cdot \vec{\pi}) \quad , \quad [5]$$

* For symbols see GLOSSARY

and (Happel and Brenner, 1965a)

$$\underline{\underline{B}} = \left[- \int_S dS \cdot \underline{\underline{P}} \right]^{-1} \quad [6]$$

where $\underline{\underline{\pi}}$ and $\underline{\underline{P}}$ are respectively the stress diadic and triadic related to the field of flow. Thus, the knowledge of this field is a prerequisite to the solution of the equations of motion.

Scientific background and previous studies

A. Mobility, Forces, and Torques

The aerodynamic force and torque acting on particles embedded within an arbitrary field of flow near a collecting wall has been theoretically calculated and experimentally determined for a few types of cases.

There is a limited number of studies concerning a motion of a spherical solid particle (Brenner, 1965; Brenner, Goldman, and Cox, 1967; Gallily and Mahrer, 1973), and even less concerning a motion of spheroids (Wakiya, 1959) or cylinders (De Mestre and Russel, 1975), which take care of the effect of the wall. The overwhelming majority of investigations were devoted to the study of the fluiddynamic force and torque which operate on isolated particles, assuming that the interaction between the latter and the wall can be neglected. In these studies, the field of flow was characterized by the creeping motion conditions

$$Re_t = L_c |\underline{\underline{v}}| / \nu \ll 1 \quad [7]$$

and

$$Re_r = L_c^2 |\underline{\underline{\omega}}| / \nu \ll 1 \quad [8]$$

where ℓ is a typical length of the particle, ω is the rotational velocity, and ν is the kinematic viscosity.

1. Motion of isolated particles in a continuous-regime

a. Ellipsoids

Considering the case of relatively large particles for which Knudsen number Kn is $Kn (\equiv \bar{\lambda} / \ell) \ll 1$, one has for a steady motion of an isolated ellipsoid within an arbitrary flow \underline{v} (Brenner, 1964)

$$\underline{F}_F = \mu \underline{K} \cdot [\langle \underline{v}_M + \frac{1}{3!} (D^2 \underline{v})_M + \frac{1}{5!} (D^4 \underline{v}) + \frac{1}{7!} (D^6 \underline{v})_M + \dots \rangle - \underline{u}_M] \quad [9]$$

and

$$\underline{L}_{M,F} = \mu \underline{Q} \cdot [\langle (\underline{\Omega} \times \underline{v})_M + \frac{3!2}{5!} (D^2 \underline{\Omega} \times \underline{v})_M + \frac{3!3}{7!} (D^4 \underline{\Omega} \times \underline{v})_M + \frac{3!4}{9!} (D^6 \underline{\Omega} \times \underline{v})_M + \dots \rangle - (a_{i+1}^2 + a_{i+2}^2) \underline{\omega}] \quad [10]$$

where \underline{K} , the translation tensor, is

$$\underline{K} = 16\pi a_1 b_1 c_1 \left(\frac{i \ i}{x_0 + a_1^2 \alpha_0} + \frac{j \ j}{x_0 + b_1^2 \beta_0} + \frac{k \ k}{x_0 + c_1^2 \gamma_0} \right); \quad [11]$$

\underline{Q} is

$$\underline{Q} = \frac{16\pi a_1 b_1 c_1}{3} \left(\frac{i \ i}{b_1^2 \beta_0 + c_1^2 \gamma_0} + \frac{j \ j}{c_1^2 \gamma_0 + a_1^2 \alpha_0} + \frac{k \ k}{a_1^2 \alpha_0 + b_1^2 \beta_0} \right) \quad [11A];$$

$$x_0 = a_1 b_1 c_1 \int_0^\infty d\lambda / \Delta; \quad \alpha_0 = a_1 b_1 c_1 \int_0^\infty \frac{d\lambda}{(a_1^2 + \lambda) \Delta}; \quad \beta_0 = a_1 b_1 c_1 \int_0^\infty \frac{d\lambda}{(b_1^2 + \lambda) \Delta};$$

$$\gamma_0 = a_1 b_1 c_1 \int_0^\infty \frac{d\lambda}{(c_1^2 + \lambda) \Delta}; \quad \Delta = [(a_1^2 + \lambda)(b_1^2 + \lambda)(c_1^2 + \lambda)]^{1/2};$$

$$D^2 = a_1^2 \partial^2 / \partial x^2 + b_1^2 \partial^2 / \partial y^2 + c_1^2 \partial^2 / \partial z^2;$$

$\square = \sum_{i=1}^3 \alpha_i^2 \partial/\partial x_i' + \sum_{j=1}^3 \beta_j^2 \partial/\partial y_j' + \sum_{k=1}^3 \gamma_k^2 \partial/\partial z_k'$; $\alpha_i, \beta_j, \gamma_k$ are the ellipsoid's semi-axes; and $i = 1, 2, 3$ stands respectively for a, b, c , in a cyclic order.

For a non-steady motion of an isolated particle in an arbitrary non-steady field, one has to take into account an "added mass" and "added moment of inertia" (Lamb, 1932), an "added buoyancy", and relaxation effects resulting from the changing relative velocity between the particle and the fluid (Morrison, 1974). The "added mass" and "added moment of inertia" which have to be combined with the mass and moment of inertia of the particle, respectively, are proportional to the density of the displaced fluid, the proportionality factor being of the order of unity. So, for aerosol systems they can be neglected. On the other hand, the so called Basset-term, related to the fluid-relaxation effects has yet to be checked for non-spherical particles.

In the case of an isolated solid sphere, for example, the most general expression of the fluiddynamic resistance F_F is (Morrison, 1974a)

$$F_{F,i} = m' (Dv_i/Dt - \gamma \nabla v_i) - (m'/2) (Du_i/Dt - \partial v_i/\partial t - u_j \partial v_i/\partial x_j) - 6\pi\mu a (u_i - v_i) - \frac{6\pi\mu a^2}{(\pi\gamma)^{1/2}} \int_{-\infty}^t \frac{(du_i/dt_1 - \partial v_i/\partial t_1 - u_j \partial v_i/\partial x_j) dt_1}{(t-t_1)^{1/2}} \quad [12]$$

where a_0 is the radius, m' is the mass of the displaced fluid, and D/Dt is the substantial derivative operator. Thus, the introduction of [12] into the equation for the creeping translational motion of even a solid sphere, would turn the last equation into an integro-differential one. This

introduction has been never done due to the enormous complications it brings to the equations of motion [1]-[2] for even the simple spherical particle.

Here it should be remarked about the suitability of an ellipsoid to simulate the shape of real particles. Approximating the shape of the latter by that of regular bodies, one can distinguish among categories, as given in Table 1.

Shape	Percent by Weight in sample		Particles (larger than 0.1 m)
	Range	Average	
Spherical	0-20	10	Smoke, pollen fly-ash
Irregular	10-90	40	Mineral
Cubical			Cinder
Flakes	0-10	5	Mineral epidermis
Fibrous	3-35	10	Lint plant fibers
Condensation flocs	0-40	15	Carbon, smoke fume

Table 1: Airborne Dust Particle Shapes (Stern, 1968)

(^{*} Also, asbestos fibers and cloud ice crystals).

In this category system, a cylindrically shaped particle (fiber, needle) may be looked upon as a prolate rotational ellipsoid of a very large polar to equatorial axis ratio or a finite slender body. A discoid-type particle (flake) may be envisaged as an oblate rotational ellipsoid of a very small axial ratio, and a straight-chain condensation floc of spherical primary particles may be roughly considered as a rod.

For the asymptotic forms of the cylinder and the disk, one has instead of Eqs. [9] and [10] somewhat simpler equations relating κ and Q to the axial ratio of the body (Brenner, 1965a; Gallily, 1975).

b. Regular bodies with planar surface sections

There is no theoretical solution for the fluiddynamic resistance force and torque acting on particles having planar surface sections such as cubes, etc. (Brenner, 1965b; all studies of these particles have been empirical (Heiss and Coull, 1952; Pettyjohn and Christiansen, 1948 ; Jayaweera, 1969; Kajkawa, 1971; Horwath, 1974; Walkenhurst, 1976). Heiss and Coull (1952), for example, defined an empirical factor G relating the rate of fall a non-spherical particle to that of a volumetrically equivalent sphere of diameter d_s , by

$$u_{\infty} = (2 \rho_p g d_s^2 / 18 \mu) G \quad [13]$$

for a flatwise fall and constant circularity d_s/d_n , where d_n is the diameter of a circle equal to particle's cross section perpendicular to its motion, they found

$$\log_{10} G = \log_{10} (d_s \psi^{1/2} / d_n) - 0.25 \psi^{1/2} d_s / d_n, \quad [14]$$

and for an edgewise fall and a variable circularity,

$$\log_{10} G = \log_{10} (d_s \psi^{1/2} / d_n) - [0.270 / \langle \psi^{1/2} (d_s / d_n)^{0.345} \rangle] \quad [15]$$

in which ψ , the sphericity factor, is $\psi = \pi d_s^2 / s$ and s is the surface of the particle.

The relationship between G and K_{ii} is given by

$$K_{ii} = (3 \pi / 2 \mu G) d_s \quad [16]$$

It should be remarked that no empirical formula is available for the rotational mobilities of the discussed bodies.

2. Motion of isolated particles in the molecular regime

The mobility of aerosol particles in creeping motion and the molecular regime where $K_n \gg 1$ has been calculated for a rigid sphere (Epstein, 1924), and later for nonspherical particles of a cylindrical, discoidal, spheroidal and cubical shape (Dahneke, 1973a; Schwartz, 1976). Dahneke's general equation for the resistance force in a direction characterized by the cosines α', β', γ' with respect to the velocity u_n is

$$\begin{aligned} F_n^* = & (\mu u_n / L_c K_n^*) \int_S [2 - f + (\pi/4) f (T_s / T)^{1/2} \alpha \alpha' \\ & + (1/2) f \beta \beta' + (1/2) f \gamma \gamma'] dS \end{aligned} \quad [17]$$

* A general formula only.

where L_c is a characteristic length, $K_n' = \bar{\lambda}/L_c$, and f is the fraction of gas molecules reflected diffusely with a temperature accommodation coefficient of 1.

3. Motion of isolated particles in the continuum-slip regime

Aerosol particles in many natural and man-made systems have sizes characterized by $0 < Kn < 0.2$; however, there are but a few studies of mobility of nonspherical particles in this Knudsen-number range. In analogy with the case of two rigid spheres (Morrison, 1974b) in which the slip boundary condition on their surface is taken to be

$$v_t = C_m (\bar{\lambda}/\mu) \sigma_t \quad [18]$$

where $C_m \approx (2-f)/4$ and σ_t is the tangential stress on the surface, one can assume that a resistance tensor \tilde{K} calculated for a nonspherical particle on a continuous fluid assumption can be adjusted for the continuum-slip regime by multiplying it by a factor α which depends on Kn and C_m alone,

$$\tilde{K}_{adj} = \tilde{K}_{con} \cdot \alpha(Kn, C_m) \quad [19]$$

The mobility of non-spherical particles in the continuum-slip regime was calculated by a semi-empirical technique (Dahneke, 1973). In this technique one finds first a sphere of radius R having the same ratio of resistances in the continuous and molecular regime as that of the particle in question; then, assuming that sphere to have also the same ratio of the continuous-regime resistance to the resistance at any Knudsen number as that of the nonspherical particle, one deduces from the equation

$$K_{nR}/K_n^i = L_c/R$$

and the typical length L_c the appropriate $K_{nR}(\bar{\lambda}/R)$ and calculates the mobility of the nonspherical particle by

$$B = B_{con.} (1 + A_1 K_n + A_2 e^{-A_3/K_n}) \quad [20]$$

In the experimental side, the translational mobility in the continuum-slip regime was studied at our laboratories (Gallily, 1975) for cylinders sedimenting at an atmospheric pressure.

B. Deposition

A directed study of deposition of nonspherical particles on various obstacles has not been performed until recently when Gallily and coworkers (Gallily, 1975), and Gentry and Spurny (1976) have started investigations.

The rate of sedimentation, however, has been used for quite a time as a means for size characterization through the concept of the Stokes (R_s) or the Aerodynamic (R_a) Radius (Fuchs, 1964; Stöber, 1972; and others) respectively defined by

$$R_s = (9\mu |u_{\infty,z}| / 2|g|s_r)^{1/2}$$

or

[21]

$$R_a = (9\mu |u_{\infty,z}^0| / 2|g|s_r)^{1/2}$$

where $u_{\infty,z}^0$ is the experimentally measured vertical settling velocity.

1. Aerodynamic radius studies

Studies on the aerodynamic radius of nonspherical bodies were carried out for aggregates of spherical latex aerosol particles of various configurations and for asbestos fibers, mainly by the aid of the Stöber spectrometer (Stöber, 1972), and for variously shaped irregular aerosol particles (Kotrappa, 1972), all in an atmospheric pressure and Knudsen numbers of $Kn < 0.2$, approximately. Also, aerodynamic radii of aerosol latex aggregates have been determined at reduced pressures, i.e. higher Knudsen numbers (Hochrainer and Hanel, 1975).

Experiments on the rate of sedimentation of (model) cylinders, ellipsoids, cubes etc. in liquids at creeping flow conditions, have been carried out lately too (Morvath, 1974; Walkenbörst, 1976).

These studies were concerned with isolated particles falling far removed from walls; no study was dedicated to investigate the aerodynamic effect of the wall. The result for aerosol particle systems, where obviously no ideally regular bodies could be produced, were expressed in the form of empirical equations related, in the case of linear aggregates and fibers, to the theoretical continuous-regime equation and incorporating a Cunningham-like correction factor.

2. Diffusional transport

The diffusional transport of nonspherical particles was theoretically studied by Brenner (1972) by treating an ensemble rather than individual bodies.

3. Stochastic motion of single particles

The sedimentation in still air of nonspherical particles in the micron-size range was studied theoretically by a Monte Carlo technique (Gallily, 1975; Gallily and Cohen, 1976) in which only regular shapes such as cylinders, disks, and rotational ellipsoids, were treated. In this study the probability density function for an orientation change of a single sedimenting particle was taken to be (Gans, 1928)

$$P(X, t) = \sum_{n=0}^{\infty} \frac{2n+1}{2} e^{-n(n+1)D_R t} P_n(X) \quad [22]$$

where $X = \cos \theta$ and $P_n(X)$ is Legendre's polynomial of degree n .

The results, expressed in terms of an aerodynamic radius R_a and its square R_a^2 which is proportional to $|u_{\infty, z}|$, showed that:

- a. The vertical velocity of sedimentation during a time T_1 has an inherent scatter of values;
- b. The average aerodynamic radius of a cylinder is somewhat higher than that of a unit density sphere having a radius equal to the equational axis of the former;
- c. The standard deviation of the distributions of R_a and R_a^2 bounded by the values appropriate to a flatwise and edgewise fall, is between 0.5% and 12% of the average;
- d. The standard deviation for cylinders, for example, increases with the aspect ratio (= length over diameter) of the particle;

- e. The average velocity of sedimentation of cylinders, for example, does not change with T_1 , but the standard deviation decreases with it.
- f. The "initial history" of the particle is forgotten by it after times of sedimentation of the order of a few seconds.

II. STATEMENT OF AIM OF REPORTED STUDY

In view of the existing background knowledge, we have decided to conduct a research along the following lines:

1. Mobility

a. Continue with the experimental determination of the principal resistance coefficients of cylindrical aerosol particles at reduced pressures, thus increasing the upper limit of the Knudsen number of our aerosol system and treating smaller atmospheric particles.

b. Investigate experimentally the resistance coefficient of cubical aerosol particles in the micron size-range.

2. Deposition in still air

a. Study experimentally deposition in still air of cylindrical aerosol particles, and compare it with the theoretical Monte Carlo calculations of Gallily and Cohen (1976).

b. Continue the Monte Carlo theoretical calculations (Gallily and Cohen, 1976) for regularly-shaped nonspherical particles so as to find the spatial scatter of sedimentation points on an horizontal plane.

III. EXPERIMENTAL

Mobility

A. Cylindrical Aerosol Particles

The mobility coefficients of cylindrical aerosol particles at a reduced pressure were experimentally investigated in the same way as that used for their determination at an atmospheric one (Gallily, 1975).

1. Apparatus, particles, and procedure

The apparatus employed for this purpose was essentially the same as that used earlier (Gallily, 1975) but for the incorporation of a vacuum system attached to the sedimentation cell and glass capillary air bleeders for the slow introduction of the aerosol particles to be determined (Figs. 1 through 4, and photograph 1).

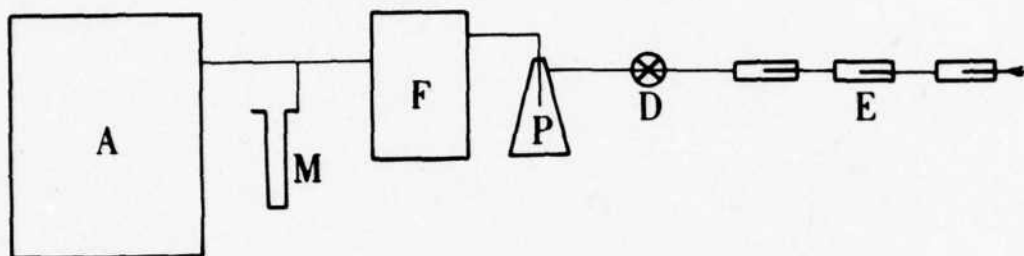


Fig. 1. The experimental set-up for mobility determination.

F - stereo-sedimentation cell, P - glass fibers' container,
E - three aerosol introduction bleeders, A - vacuum system (pump,
traps), M - manometer, D - stopcock

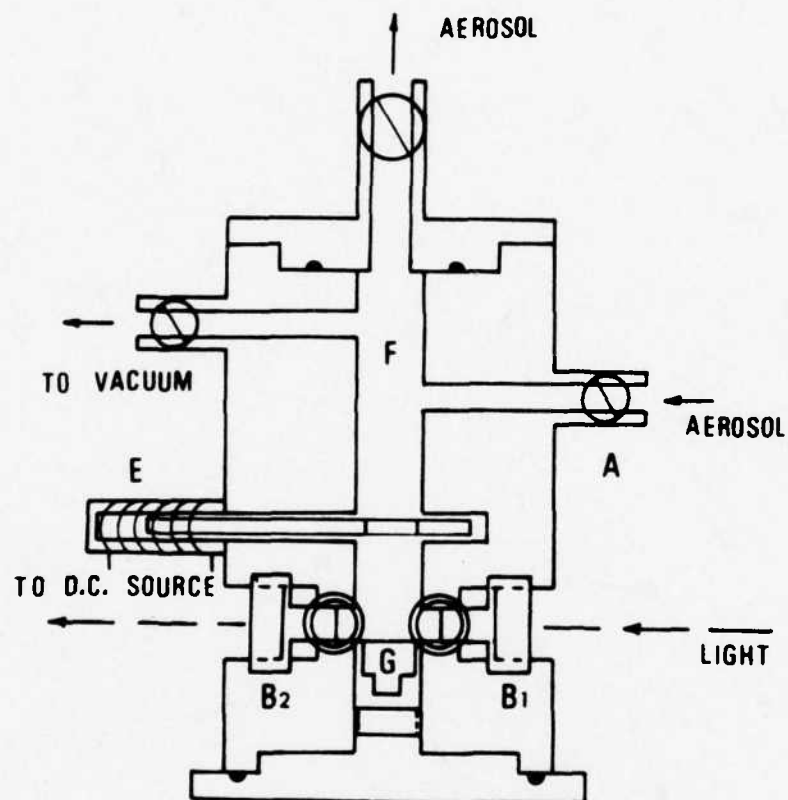


Fig. 2. The stereo-sedimentation cell (vertical cross-section)

F - cylindrical sedimentation cavity, G - scanning electron microscope stub, B₁, B₂ - viewing microscopes' port holes, E - Blocking, electromagnetically activated rod.

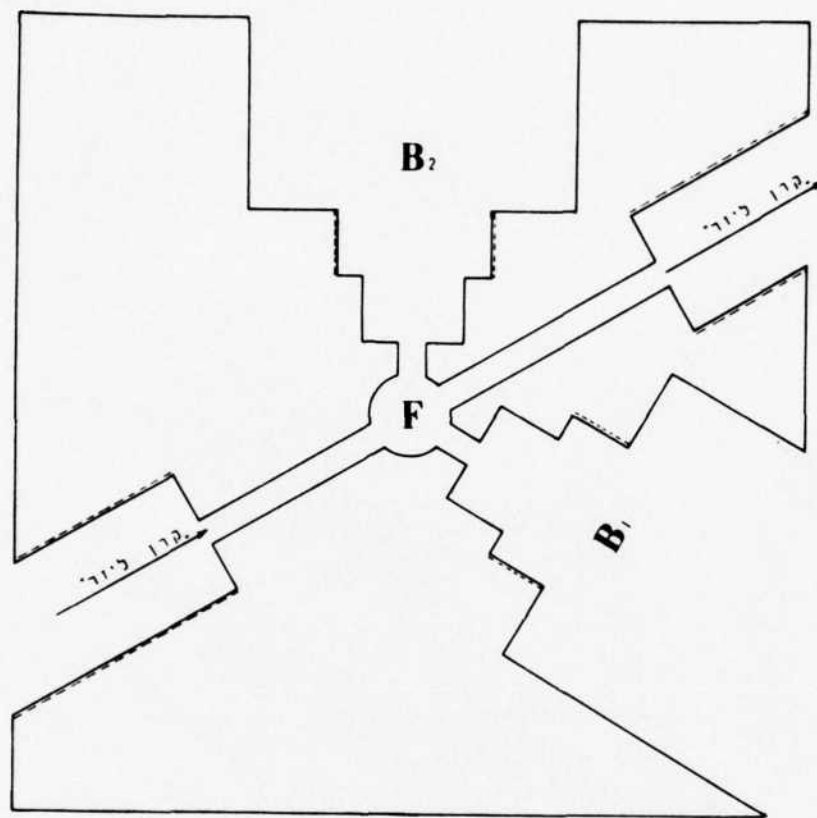


Fig. 3. The stereo-sedimentation cell (horizontal cross-section at port-holes' level).

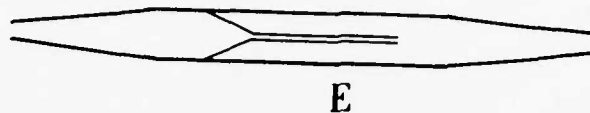
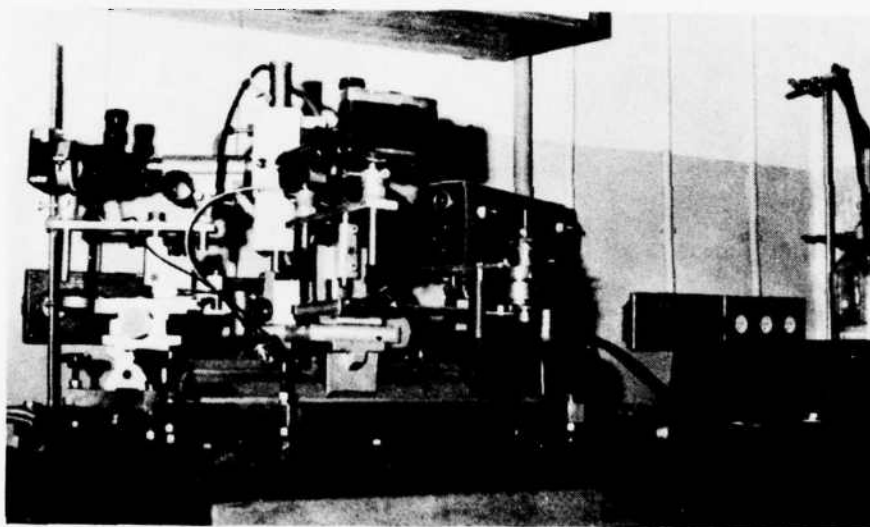


Fig. 4. Introduction-bleeder glass tube.

E - glass capillary.



Photograph 1. The mobility sedimentation cell, microscope-cameras, light source, and light-chopper / frequency-counter combination.

The particles were glass fibers having lengths of 5-50 and diameters of 0.3-1.5 . These were produced from a Whatman GF/C Filter Paper raw material (Whatman, England) by an electric grinder, and dispersed by a shaking action as described earlier (Gallily, 1975). Their density at room temperature according to the literature was 2.23 g.cm^{-3} , which was experimentally checked by us and found to be correct within $\pm 5\%$.

The experimental procedure adopted consisted of the same preliminary steps of system levelling and calibration as used in the atmospheric pressure determinations, evacuation of the sedimentation cell F and the glass fiber container P (Fig. 1) till a pressure of about 300 mm Hg, and finally a slow controlled introduction into the cell of the outside air which picked up fiber particles during its passage through P . The trajectories of the particles falling into the lower section of F (Fig. 2) were photographed as before from two directions of sight, the location of the sedimented particles was found by the same technique reported earlier (Gallily, 1975), and the size determination was performed in a scanning electron microscope (Stereoscan, Mark IV, Cambridge, England) by our photogrammetric method (Gallily, 1975). The resistance coefficients pertaining to motion perpendicular ($K_{\perp} \equiv K_{11}$) and parallel ($K_{\parallel} \equiv K_{33}$) to the cylinder's axis were calculated according to the mathematical analysis developed by us (Gallily, 1975).

Here, in the size analysis of the particles, however, they were not gold-shadowed on the stubs and so no uncertainty was introduced into the measurement of their binary dimensions.

2. Results

The results are given in Table 1 and Fig. 5 in the form of the translational resistance coefficients $K_1 (\equiv K_{11})$ and $K_3 (\equiv K_{33})$ for various values of cylinder's length ℓ and diameter c at reduced pressures. K_{11} is the resistance coefficient related to transverse motion while K_{33} is the coefficient related to a longitudinal one, as given by the diagonalized translation tensor

$$\underline{\underline{K}} = \underline{\underline{ii}} K_{11} + \underline{\underline{jj}} K_{22} + \underline{\underline{kk}} K_{33} \quad [23]$$

the theoretically calculated values, $K_{ii,t}$, are based on the continuous fluid equations (Happel and Brenner, 1965b)

$$K_{11} = K_{22} = \frac{4\pi\phi}{\ln 2\phi + 1/2} c \quad [24]$$

and

$$K_{33} = \frac{2\pi\phi}{\ln 2\phi - 1/2} c \quad [25]$$

where $\phi = \ell/c$.

O.N	l (μm)	c (μm)	l/c	$K_{11,ex} \times 10^3$ (cm)	$K_{33,ex} \times 10^3$ (cm)	$K_{11,t} \times 10^3$ (cm)	$K_{33,t} \times 10^3$ (cm)	P (mm Hg)	t($^{\circ}\text{C}$)
1	58.2	0.87	67	23.1	17.5	13.6	8.3	370.8	20.3
2	24.7	0.39	63	2.2	1.5	5.8	3.6	370.6	21.7
3	11.1	0.82	14	5.5	4.1	3.7	2.5	379.0	22.8
4	17.0	1.08	16	7.8	6.6	5.4	3.6	403.0	21.2
6	44.6	0.75	60	16.4	9.6	10.6	6.5	354.0	21.6
7	8.9	0.53	17	2.6	1.6	2.8	1.8	342.0	25.0
8	25.1	0.50	50	4.6	3.8	6.2	3.8	426.0	26.2
9	19.7	1.67	12	29.6	20.8	6.8	4.6	336.0	28.3
10	5.9	0.80	7	3.2	2.1	2.3	1.7	344.0	28.3
11	46.2	1.15	40	27.7	19.4	11.9	7.5	319.0	24.9
12	21.3	0.83	26	7.9	6.6	6.0	3.9	346.0	28.1
13	40.4	0.40	101	2.1	1.2	8.7	5.3	328.0	26.7
14	14.8	1.53	10	23.5	14.2	5.4	3.8	317.0	29.3
15	13.7	1.14	12	5.8	4.9	4.7	3.2	321.0	28.9
16	22.9	1.19	19	24.1	22.0	6.9	4.6	325.0	29.5
17	18.9	1.13	17	24.1	11.8	5.9	3.9	124.0	29.3
18	58.3	0.87	67	14.5	9.3	13.6	8.3	126.0	29.3
19	38.2	0.73	52	10.9	7.0	9.3	5.7	122.0	28.0

Table 1: The translational resistance coefficients of a cylinder at reduced pressures.

$K_{ii,ex}$ - experimentally based value; $K_{ii,t}$ - continuous regime theoretical value.

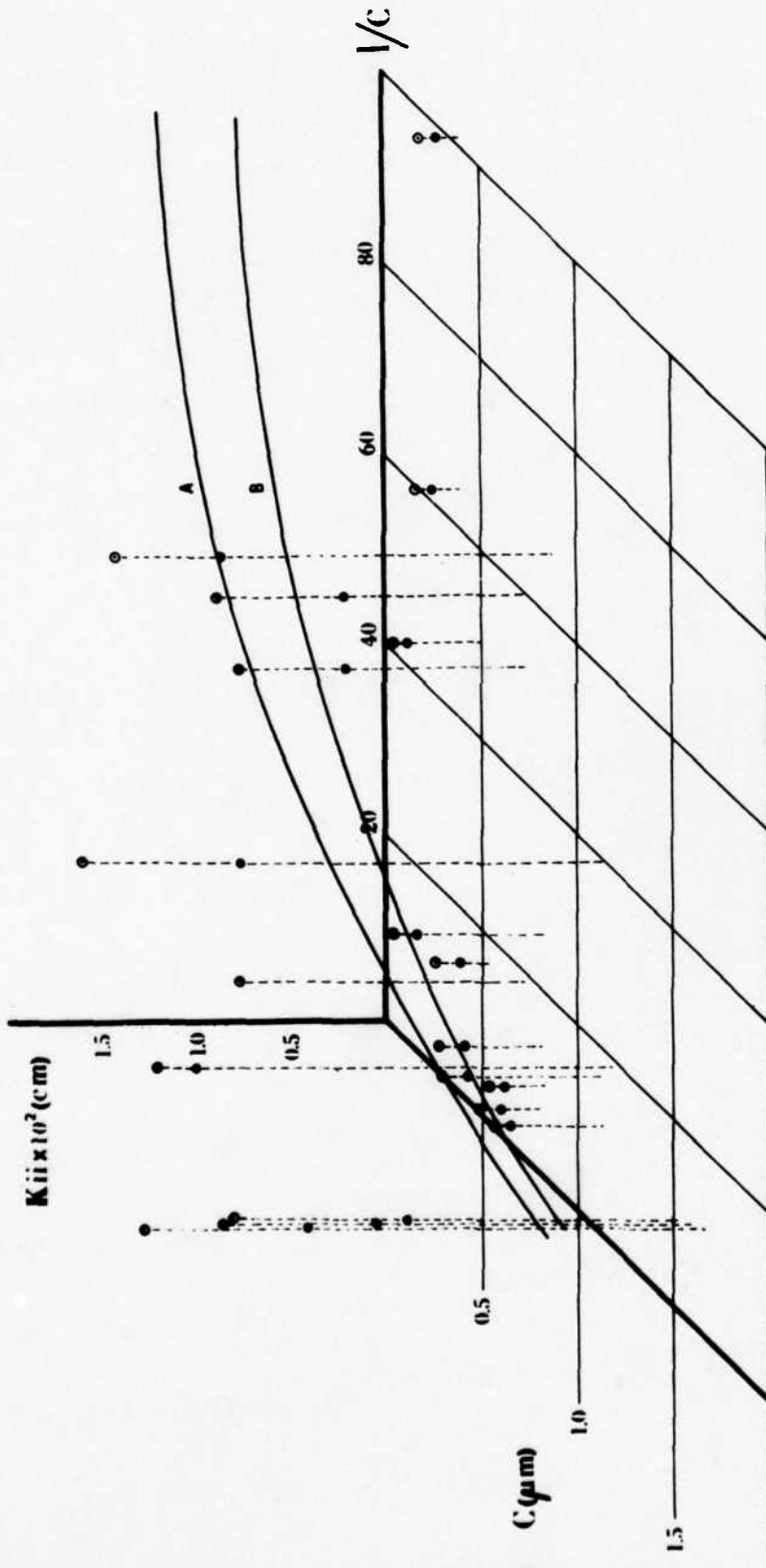


Fig. 5. The translational resistance coefficients of a cylinder at

reduced pressures.

\circ - $K_{11,ex}$, \bullet - $K_{33,ex}$; A, B - regressed lines related to K_{11} and K_{33} , respectively.

3. Analysis and discussion

The experimentally determined resistance coefficients were compared to three sets of calculated values (Table 2) pertaining to:

a. Continuous fluid coefficients,

which were apriori expected to be higher than the experimental ones due to the neglect of the Knudsen number effect

b. Continuous fluid coefficients for short cylinders in which

correction was made for the blunt edges, i.e. finite length, of the latter

c. Slip-continuum regime coefficients for a transverse motion of an infinite cylinder.

The corrected resistance coefficients were calculated on the basis of Heiss and Coull's study (1952) in which the coefficients were expressed in terms of the empirically determined constant G defined by Eq. [13] and related to K_{ii} by Eq. [16].

Thus, to estimate the effect of the blung edge of a finite cylinder on its translational resistance, one can use Eq. [16] and compare the coefficients K_{ii} of the cylinder and a prolate ellipsoid of the identical dimensions according to

$$K_{ii,cy.}/K_{ii,ell.} = (G_{cy.}/G_{ell.})(d_{s,cy.}/d_{s,ell.}) \quad [26]$$

in which the right hand bracketed ratios are for bodies of the same axial and transverse dimensions. From Heiss and Coull's study, it appears that $G_{cy.} / G_{ell.} = 1.06$ for $l/c = 5$ and that it approaches 1 for a higher length to diameter ratio. Thus,

$$(K_{ii,cy} / K_{ii,ell.}) \cong (d_{s,cy.} / d_{s,ell.}) = \left[\frac{\pi (c/2)^3 \ell}{(4\pi/3) (c/2)^2 (\ell/2)} \right]^{1/3} = 1.5^{1/3} \quad [27]$$

which is the actual correction factor used by us.

From Tables 1 and 2, it is seen that:

a. The translational resistance coefficients of the cylinder at reduced pressures ($K_n \leq 0.16$) are of the same order of magnitude as those calculated on a continuous medium basis.

b. The coefficients for cylinders of a diameter above $1 \mu m$, approximately, are greater than the calculated ones $K_{u,t}$, whereas those related to cylinders of diameters below $0.5 \mu m$, approximately, are smaller than $K_{u,t}$.

The obvious deduction to arise was that the effect of fluid discontinuity ($K_n > 0$) is noticeable. So to check this effect, the resistance to the transverse translation of a cylinder was compared with the theoretical equation of Pich (1967) in which the Knudsen number influence for the slip-continuum regime has been taken into account

$$F_{F,1} = \frac{4\pi\mu U}{2.0022 - \ln R_{e_1} + 1.747 K_{n_1} - \ln(1 + 0.749 K_{n_1})} \quad [28]$$

O.N.	ℓ (μm)	c (μm)	ℓ/c	$\frac{K_{11,ex}}{K_{11,t}}$	$\frac{K_{33,ex}}{K_{33,t}}$	$\frac{K_{11,ex}}{K_{33,ex}}$	$\frac{K_{11,t}}{K_{33,t}}$	$K_{11,e} \times 10^3$ (cm)	$K_{33,e} \times 10^3$ (cm)	$\frac{K_{11,ex}}{K_{11,e}}$	$\frac{K_{33,ex}}{K_{33,e}}$
1	58.2	0.87	67	1.70	2.10	0.76	0.61	15.53	9.55	1.49	1.84
2	44.6	0.75	60	1.55	1.47	0.59	0.62	12.16	7.50	0.33	0.37
3	24.7	0.36	63	0.37	0.43	0.70	0.62	6.65	4.09	1.35	1.26
4	11.1	0.82	14	1.48	1.64	0.75	0.68	4.21	2.84	1.30	1.28
5	17.1	1.08	16	1.45	1.82	0.84	0.67	6.20	4.14	1.26	1.59
6	8.3	0.83	10	0.98	1.02	0.73	0.70	3.42	2.37	0.85	0.90
7	8.9	0.53	17	0.95	0.87	0.61	0.67	3.18	2.11	0.83	0.76
8	25.1	0.50	50	0.74	0.99	0.83	0.62	7.08	4.40	0.65	0.87
9*	19.7	1.67	12	4.38	4.48	0.70	0.69	7.74	5.29	3.83	3.94
10	5.9	0.80	7	1.37	1.21	0.64	0.73	2.64	1.90	1.20	1.08
11	46.2	1.15	40	2.34	2.60	0.70	0.63	13.59	8.54	2.04	2.27
12	21.3	0.83	26	1.31	1.69	0.83	0.65	6.90	4.45	1.14	1.48
13	40.4	0.40	102	0.24	0.23	0.58	0.60	10.01	6.05	0.21	0.20
14*	14.8	1.53	10	4.37	3.77	0.61	0.70	6.15	4.28	3.82	3.32
15	13.7	1.14	12	1.23	1.53	0.85	0.69	5.34	3.65	1.08	1.34
16*	22.9	1.19	19	3.47	4.82	0.91	0.66	7.94	5.22	3.03	4.22
17*	18.9	1.13	17	4.07	2.99	0.49	0.67	6.78	4.50	3.56	2.62
18	58.3	0.88	67	1.07	1.12	0.64	0.61	15.53	9.53	0.94	0.98
19	38.3	0.73	52	1.16	1.18	0.60	0.62	10.69	6.63	1.42	1.40

Table 2. Comparison of resistance coefficients of a cylinder at reduced pressures.

$K_{ii,ex}$ - experimental values; $K_{ii,t}$ - continuous fluid values;

$K_{ii,e}$ - corrected, calculated values.

where F_{r_1} is the resistance per unit length, $K_{n_1} = \bar{\lambda}/c$ and $Re_1 = 121 c/\nu$.
According to Eq. [28],

$$K_{11} = \frac{4 \pi \ell}{2.0022 - \ln Re_1 + 1.747 K_{n_1} - \ln(1 + 0.749 K_{n_1})} \quad [29]$$

for a very long, essentially infinite cylinder.

The comparison of Eq. [29] with the results of both the atmospheric (Gallily, 1975) and the reduced pressure experiments is presented in Table 3, from which it can be observed that for cylinder's diameters above $0.5 \mu m$, Pich's values are lower than the experimental and the continuous fluid calculated ones whereas for diameters below $0.5 \mu m$ the former approaches the experimental coefficients.

To smooth out the fluctuations in the determined coefficients K_{ij} , a regression of their values was made along the pattern of the continuous fluid expressions (Eqs. [24] and [25]) as the theoretical treatment leading to those equations was expected to be essentially valid. In the regression, K_{ij} values marked in Table 2 by an asterik were not taken into account according to a statistical test.

The results are formulated by

$$K_{11} = 1.31 \frac{4 \pi \phi}{\ln 2 \phi + 1/2} c \quad [30]$$

and

$$K_{33} = 1.48 \frac{2 \pi \phi}{\ln 2 \phi - 1/2} c \quad [31]$$

$\ell (\mu m)$	$c (\mu m)$	$K_{11,p}$	$K_{11,t}$	$K_{11,ex}$	$\ell (\mu m)$	$c (\mu m)$	$K_{11,p}$	$K_{11,t}$	$K_{11,ex}$
5.45	0.21	0.59	1.54	0.82	8.7	0.49	1.06	2.69	1.08
6.1	0.6	0.76	2.18	3.64	15.1	0.74	1.93	4.51	7.65
15.6	0.81	2.02	4.42	9.98	15.6	0.63	1.95	4.45	4.26
86.4	0.87	11.28	18.74	74.22	24.5	0.83	3.32	6.95	18.51
56.2	0.97	7.44	13.45	15.48			0.72	2.30	2.87
49.5	1.42	6.87	13.12	28.15			0.99	2.58	1.12
12.1	0.76	1.55	3.83	3.80	16.5	0.74	2.12	4.83	5.22
21.7	0.96	2.87	6.34	8.38	58.2	0.87	7.48	13.57	23.09
22.1	0.70	2.81	5.98	15.38	24.7	0.39	2.82	5.81	2.17
3.97	1.0	0.53	1.94	2.32	11.1	0.82	1.42	3.68	5.46
15.43	0.71	1.96	4.54	7.79	17.1	1.08	2.26	5.42	7.85
4.6	0.75	0.59	1.93	1.13	8.3	0.83	1.06	2.99	2.92
10.8	0.82	1.40	3.60	13.85	44.6	0.75	5.60	10.62	16.44
13.8	1.23	1.88	4.81	10.44	8.9	0.53	1.05	2.78	2.64
20.3	1.02	2.70	6.10	13.57	25.1	0.5	3.00	6.18	4.60
8.7	0.78	1.12	3.03	3.23	19.7	1.67	2.76	6.76	29.61
5.8	0.49	0.70	1.98	0.73	5.9	0.8	0.74	2.31	3.18
12.2	0.83	1.59	3.95	2.75	46.2	1.15	6.13	11.88	27.74
18.8	0.79	2.43	5.42	4.95	21.3	0.83	2.71	6.02	7.87
12.7	1.07	1.70	4.35	9.09	40.4	0.4	4.58	8.75	2.06
58.3	0.87	7.45	13.57	14.55	13.7	1.14	1.81	4.67	5.76
38.2	0.73	4.39	9.34	15.15	22.9	1.19	3.06	6.94	24.08
					18.9	1.13	2.38	5.93	24.13

Table 3. A comparison of Pich's and continuous fluid calculations with the experimental resistance coefficients $K_{11,ex}$ at atmospheric and reduced pressures.

$K_{11,p}$ - Pich's values; $K_{11,t}$ - continuous fluid value;

$K_{11,ex}$ - experimental value, all multiplied by 10^3 and in cm.

where $\phi = l/c$ as beforehand.

The regressed resistance coefficients are drawn vs. l/c in Figs. 6 and 7 together with the coefficients calculated according to Eqs. [24] and [25].

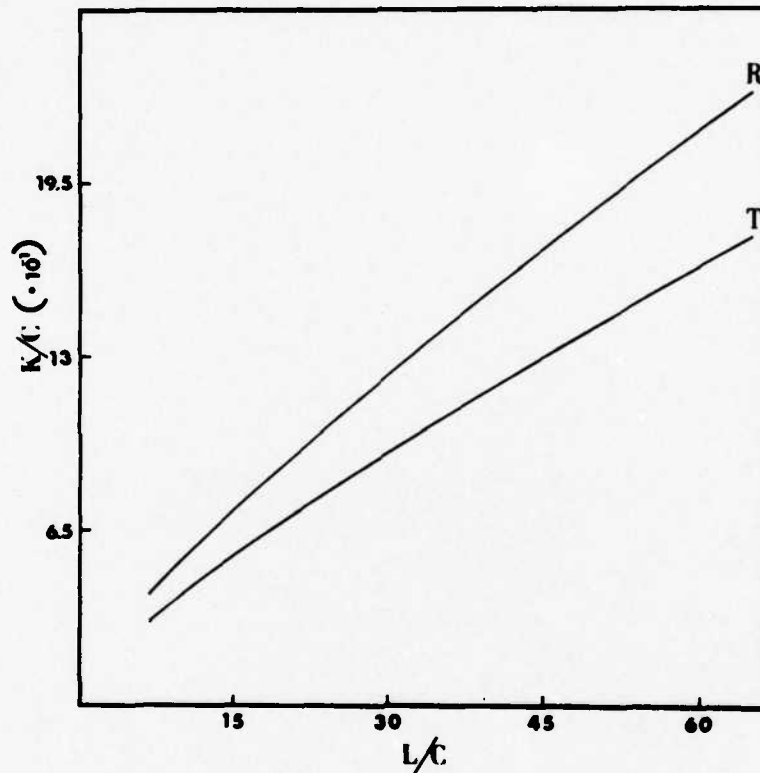


Fig. 6. The regressed, experimentally determined resistance coefficient of a cylinder in a transverse motion and reduced pressure.

R - regressed; T - continuous regime.

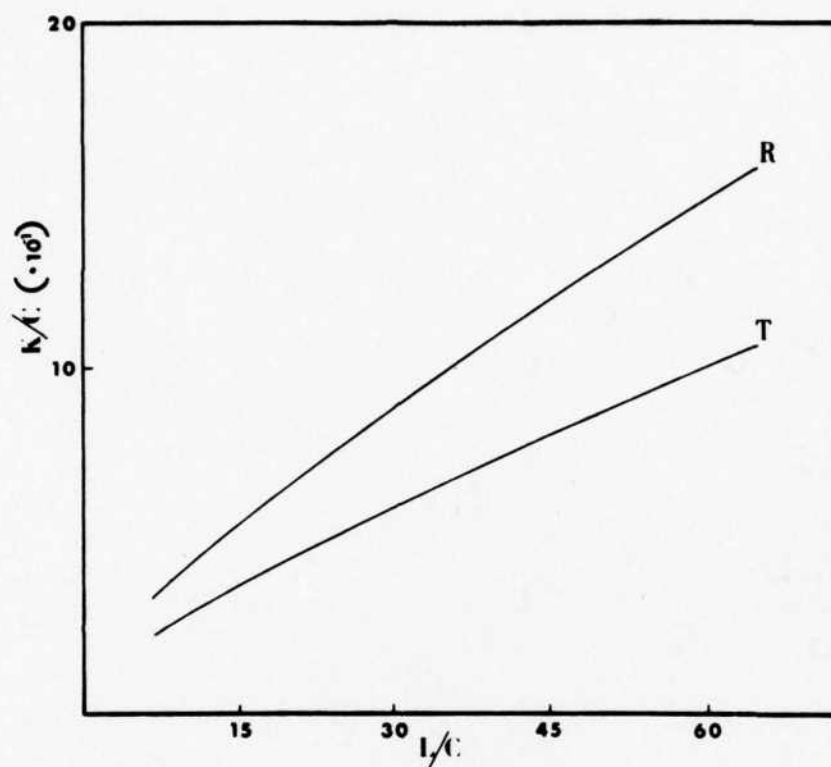


Fig. 7. The regressed, experimentally determined resistance coefficient of a cylinder in a parallel motion and reduced pressure.

R - regressed; T - continuous regime.

For comparison's sake, the equivalent regressed expressions at an atmospheric pressure, based on measurements reported earlier (Gallily, 1975), are given by

$$K_{11} = 1.48 \frac{4\pi\phi}{\ln 2\phi + 1/2} c \quad [32]$$

and

$$K_{22} = 1.79 \frac{2\pi\phi}{\ln 2\phi - 1/2} c \quad [33]$$

and Figs. 8 and 9.

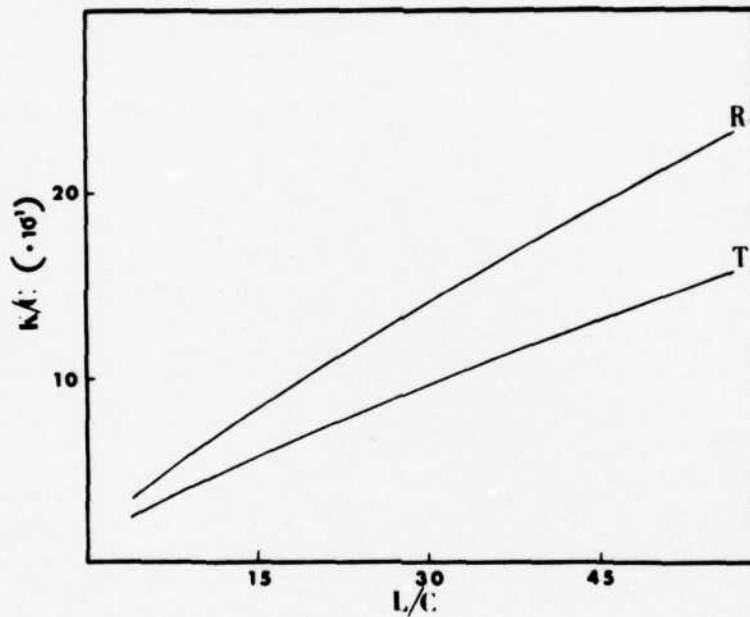


Fig. 8. The regressed, experimentally determined resistance coefficient of a cylinder in a transverse motion and an atmospheric pressure.

R - regressed; T - continuous regime.

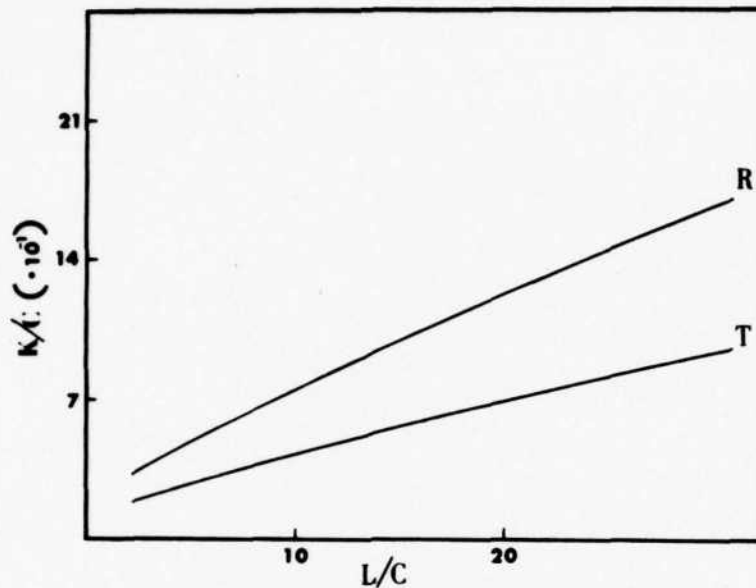


Fig. 9. The regressed, experimentally determined resistance coefficient of a cylinder in a parallel motion and an atmospheric pressure. R - regressed; T - continuous regime.

From Eqs. [30] through [32] and Figs. 6-9 it is seen again that, indeed, increasing the Knudsen's number (i.e. reducing the pressure, in our case) causes a reduction in the translational resistance coefficients, as expected.

The regressed equations can obviously serve as working formulae for the introduction of the experimentally determined tensor $\underline{\underline{K}}$ of our glass

fibers into the appropriate equation of motion of the particles. As a final remark, it should be mentioned that for the cylinders of diameters above $1 \mu\text{m}$, whose coefficients K_{ij} were found to be higher than the continuous fluid value, it was observed that none of them was of a perfect shape; furthermore, it was noticed that the less perfect was the shape, the higher was the value of K_{ij} , which leads to the idea that this may be a factor increasing the real translational resistance.

B. Cubical Aerosol Particles

The mobility of cubical aerosol particles was determined in essentially the same method as that used for the cylindrical particles. Here, however, the aerodynamic behaviour of isolated particles in a still medium is simpler than the behaviour of cylinders since, due to the symmetry of the cubical shape, the translation tensor $\underline{\underline{K}}$ can be written as

$$\underline{\underline{K}} = K \underline{\underline{I}} \quad [34]$$

where $\underline{\underline{I}}$ is the idemfactor.

Thus, under creeping flow conditions, and a quiet air, one has

$$\begin{aligned} u_{\infty, z} &= (m|g|/\mu) K^{-1} , \\ u_{\infty, x} &= u_{\infty, y} = 0 , \end{aligned} \quad [35]$$

which means that the motion is drift-free for any spatial orientation of the cube that may be changed even by the Brownian torques (Gallily, 1975).

Following Pettyjohn et al. (1948), one can express $u_{\infty,z}$ by

$$u_{\infty,z} = k_1 u_{\infty,s} \quad [36]$$

where $u_{\infty,s}$ is the Stokesian velocity of a volumetrically equivalent sphere of diameter d_s . So, denoting the side of the cubical particle by Z , one gets the relationship

$$k_1 = 18 Z^3 / K d_s^2 \quad [37]$$

in which is hidden through K the effect of the fluid discontinuity on the translational resistance.

1. Apparatus, particles, and procedure

The apparatus and method employed for the mobility determinations were the same as those used in the cylinders' case.

Though falling with no drift, the particles' trajectories were photographed, as beforehand, from two directions of sight, thus facilitating the location of each measured particle on the stub (Fig. 2) and increasing the accuracy of the velocity determination.

The particles themselves consisted of sodium chloride (Frutarom, Laboratory Chemicals, Haifa) cubes produced by a generator (Fig. 10) which was essentially a spray-drying instrument.

In this instrument, a 10% (w/w) aqueous solution of NaCl was dispersed by a two-fluid sprayer A into a 60 liter plastic drying vessel B. The sprayer was activated by filtered air which was metered by F and saturated by water

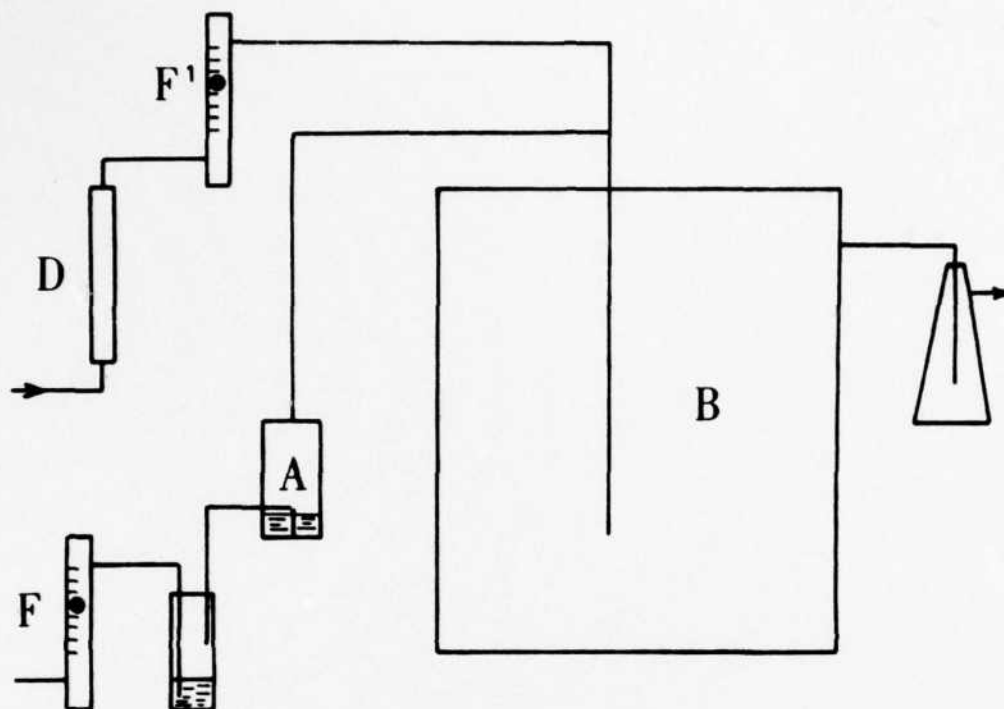


Fig. 10. The spray-drying generator.

vapour in E so that the nozzles would not get plugged by a crust of dried solid (Gallily, 1969). To evaporate the produced solution droplets, another stream of air, metered by F and dried in a SiO_2 bed D, was introduced into B. The resulting solid particles were collected in the container C and used for the mobility determination. These particles were nice cubes (Fig. 11) of an edge-dimension of $0.3\text{--}2.2\ \mu\text{m}$, which was adjusted by choosing an appropriate solution-concentration and spraying conditions.

The density of the cubes at room temperature was taken from the literature as that of the bulk value of $2.16(5) \text{ g.cm}^{-3}$; no solution filled holes within the particles were assumed because of crystallographic energetical considerations (Stöber, 1975).

The linear dimensions of three edges meeting in a corner were measured for each tested particle in the scanning electron microscope mentioned above, and by our photogrametric method (Gallily, 1975). Only particles in which any edge did not differ in length from the other two by more than 10%, were taken into consideration.

The dimensions of the cubes which stood this "perfectness test" are brought out in Table 4.



Photograph 2. A typical sodium chloride cube photographed in the scanning electron microscope. Total magnification (on the photograph) - 8460.

Concerning electrical charges on the particles, one could assume that, due to the spraying mechanism, they did exist with a distribution which was symmetrical around the zero charge; however, it was thought that these charges did not influence the settling velocity of the particles nor did they cause an increased coagulation, as could be perceived.

Another point to remark was that, as NaCl particles change to solution droplets at relative humidities of about 70% in room temperatures, they were always kept in a chemical dessicator over a SiO_2 bed.

2. Results

The translational resistance coefficients K and k_1 of cubical aerosol particles are given in Table 5 and Figs. 11-12.

Z_1	Z_2	Z_3	\bar{Z}
1.17	1.18	-	1.17
1.22	1.20	1.12	1.17
1.78	1.88	1.72	1.78
1.10	1.08	1.15	1.11
1.26	1.12	1.36	1.23
1.80	1.79	1.62	1.71
2.17	1.89	1.70	1.89
1.08	1.10	1.17	1.12
1.04	0.81	-	0.93
1.39	1.40	1.41	1.40
0.94	0.84	0.73	0.84
1.04	0.94	0.85	0.94
0.30	0.29	0.26	0.29
0.40	0.37	-	0.39
0.53	0.55	0.50	0.53
0.60	0.50	0.50	0.53
0.65	0.57	0.59	0.60
0.36	0.39	0.40	0.38
1.00	0.88	0.73	0.87
0.68	0.65	0.61	0.65
0.38	0.38	-	0.38
0.59	0.58	0.56	0.58

Table 4. The linear dimensions (in microns) of the cubes whose mobility was measured. \bar{Z} - average value .

O.N.	\bar{z} (μm)	$u_{0.9} \times 10^2$ (cm/sec)	$K \times 10^3$ (cm)	d_s (μm)	k_z	p (mm Hg)	$t(\text{c})$
1	1.17	1.74	1.09	1.45	1.26	697	23
2	1.17	1.50	1.26	1.45	1.09	697	23
3	1.78	1.35	4.93	2.21	0.42	696	27
4	1.11	1.20	1.34	1.38	0.97	693	21
5	1.23	1.34	1.64	1.53	0.89	693	22
6	1.71	1.27	4.65	2.12	0.43	698	22
7	1.89	1.38	5.77	2.34	0.38	698	22
8	1.12	0.95	1.74	1.39	0.75	700	26
9	0.93	0.85	1.12	1.15	0.98	694	24
10	1.40	0.95	3.42	1.74	0.48	699	24
11	0.84	0.61	1.16	1.04	0.84	694	22
12	0.94	0.75	1.30	1.17	0.85	694	24
13	0.29	0.52	0.06	0.36	3.11	695	24
14	0.38	0.48	0.14	0.47	3.29	698	22
15	0.58	0.45	0.51	0.72	1.34	698	22
16	0.65	0.42	0.77	0.81	0.99	696	21
17	0.87	0.38	2.03	1.08	0.50	697	22
18	0.53	0.44	0.40	0.66	1.57	695	21
19	0.39	0.19	0.37	0.48	1.24	694	21
20	0.60	0.55	0.46	0.74	1.51	694	21
21	0.38	0.40	0.16	0.47	2.75	694	21
22	0.53	0.38	0.46	0.66	1.34	694	21

Table 5. The experimentally measured resistance coefficients of translation of cubical aerosol particles.

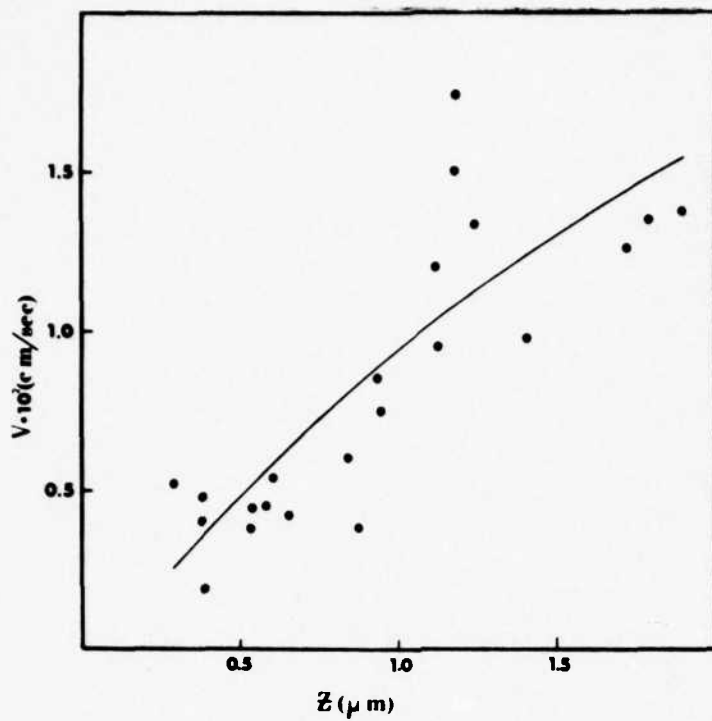


Fig. 11. The settling velocity of cubical particles vs. their linear dimension.

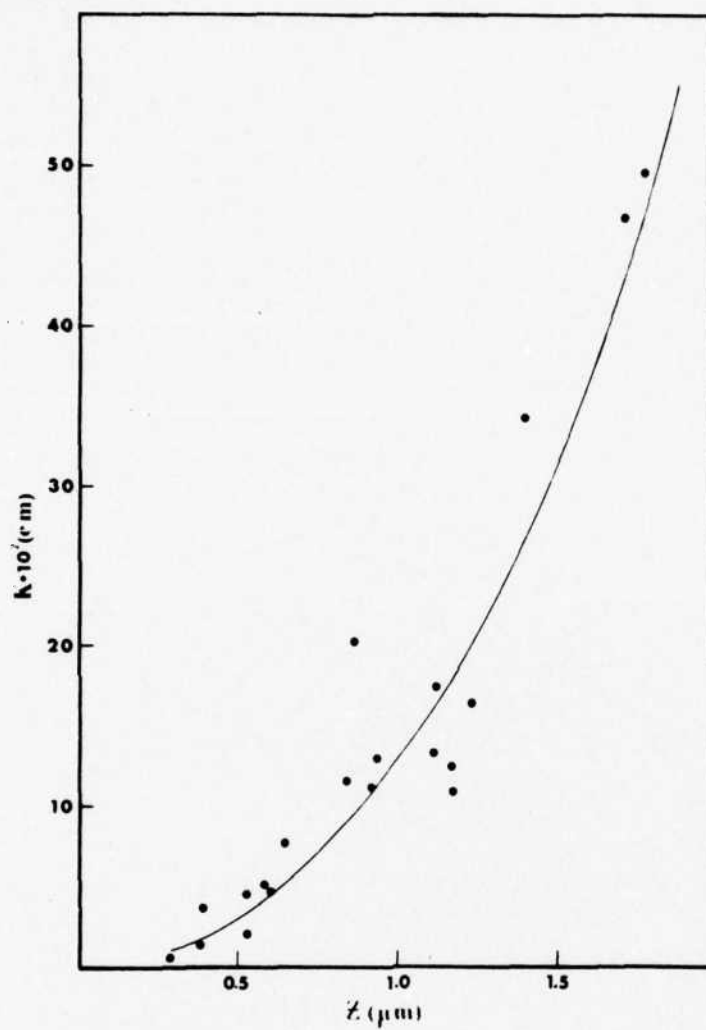


Fig. 12. The translational resistance coefficient K of cubical particles vs. their linear dimension.

3. Analysis and discussion

To smooth out the fluctuations of the experimental velocity determinations, a regression was made on the basis of

$$|u_{\infty}| = A_4 Z + A_5 Z^2, \quad [38]$$

which is shown as a full line in Fig. 11.

From the regressed values of the velocity, one could obtain a regressed expression for K (full line in Fig. 12).

The coefficient k_1 calculated according to Eq. [37], is shown in Fig. 13 together with the regression curve (full line) which is based on the velocity regression.

The k_1 curve is illustrative in comparing the relation between the settling velocity of our cubes to that of a volumetrically equivalent Stokesian sphere, as a function of Z .

It is seen that:

- a. k_1 increases with Z
- b. For $Z \leq 0.3 \mu m$, k_1 is approximately 2.8 times greater than the expected values of Heiss and Coull (1952) at continuous fluid conditions, but only 1.4 times greater if the Cunningham correction for spheres is taken into account.
- c. For $Z > 2 \mu m$, k_1 is about 2.2 smaller than the value expected from the above study of Heiss and Coull.

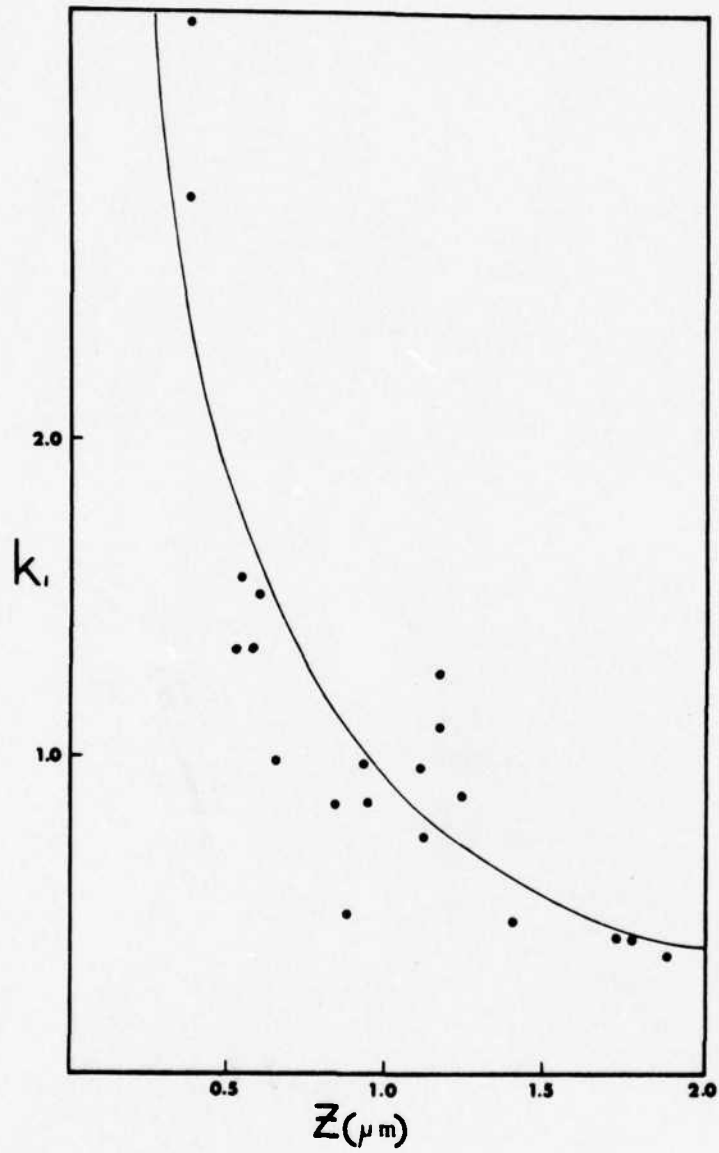


Fig. 13. The coefficient k_i of cubical particles vs. the linear dimension Z .

Here one should note that this behaviour is similar to the behaviour found in our study for cylinders.

It should be remarked that the increased resistance to motion of our cubes over the values found in liquids in earlier studies can not be quantitatively explained by assuming a particle density lower than the bulk one. No fraction of solution filled holes can account for the phenomenon; also, the external shape of the cubes was too perfect to assume that a density decrease.

One should note, however, that our cubes were not perfect bodies; so, the surface defects they show may account for an increased translational resistance at the higher end of the Z-axis (Fig. 13) whereas the medium's dielectric discontinuity (combined with the surface defects) can account for the decrease of K at the lower end of Z .

The found K values can be introduced into the equation of motion [1] to facilitate the solution of practical problems as in the cylinder case.

Deposition

The deposition of nonspherical particles in still air can be measured sometimes in situ. However, in many inaccessible systems, such as the lower parts of the human lungs, one has to infer the deposition rate from theory (Gallily, 1975; Gallily and Cohen, 1976) once the size distribution of the particles is known.

The sampling of particles with non-negligible rate of sedimentation for a size distribution analysis, is frequently performed by utilizing their settling in a quite medium on an horizontal surface.

In the case of spherical particles, one can relate the number of particles of radius r_i , n_{r_i} , sedimenting from an aerosol atmosphere in time Δt through a clean layer of thickness Δs , to their number per unit volume of the aerosol, N_{r_i} , by

$$n_{r_i} = M L N_{r_i} (|u_{\infty, r_i}| \Delta t - \Delta s) \quad [39]$$

where u_{∞, r_i} is the appropriate terminal velocity of the particles, M is the number of fields of view checked, and L is the area of each field.

For nonspherical particles the relationship is more complicated. Thus, in the cylindrical case, Eq. [39] should be replaced by

$$n_{\ell, c_i} = M L N_{\ell, c_i} \left(\sum_{\substack{u_i = u_{i, \max} \\ u_i = \Delta s / \Delta t}} P_{\ell, c_i, u_{\ell, c_i}, \Delta t} u_{\ell, c_i} \Delta t - \Delta s \right) \quad [40]$$

where $P_{\ell, c_i, u_{\ell, c_i}, \Delta t}$ is the probability that a cylinder of dimensions ℓ , and c_i will have in time Δt an average settling velocity u_{ℓ, c_i} .

This probability has been calculated by Gallily and Cohen (loc.cit).

The size distribution function, $f_{\ell, c_i} = N_{\ell, c_i} / \sum N_{\ell, c_i}$, is given now by

$$\frac{n_{e,c_i} / \left[\sum_{u_i=\Delta s/\Delta t}^{u_i=u_i, \max} P_{e,c_i, \dots} (u_i, \Delta t - \Delta s) \right]}{\sum_{e_i, c_i} \left[n_{e_i, c_i} / \sum_{u_i=\Delta s/\Delta t}^{u_i=u_i, \max} P_{e_i, c_i, \dots} (u_i, \Delta t - \Delta s) \right]} \quad [41]$$

In our experiments, we tried the technical and calculational aspects of a method based on Eq. [41].

1. Apparatus, particles, and procedure

The apparatus used to sample the particles from still air (Fig. 14) consisted of a sedimentation cell having a central cylindrical settling cavity A, a scanning electron microscope collecting stub, and two lever-activated diaphragm stops B of 0.1 mm thickness, one at a distance of 0.2 mm from the glass-covered stub and the other at a distance which could be varied between 0.3 to 2.7 mm.

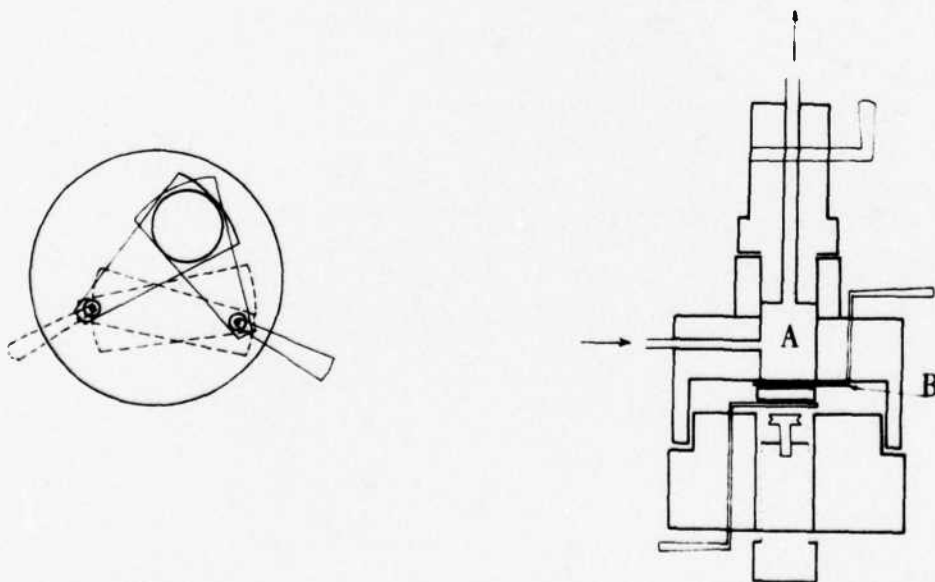


Fig. 14. The sampling cell (schematic).

The particles were glass fiber cylinders of the same origin as described above and of the same range of linear dimensions. These particles were produced by the same method cited beforehand (Gallily, 1975). The glass covered scanning microscope stubs, however, were now smeared with a thin layer of (filtered) kerosene; as a result, the cylinders which sedimented were pulled down by surface tension action towards the surface and lay flat on it, as previously ascertained also for similar sampling conditions by Gallily (1971).

The experiments themselves were conducted by introducing the glass fibers into the sampling cell with the aid of a Mariot bottle suction while the two blocking diaphragms B (Fig. 14) were shut, opening the two diaphragms at time $t=0$, and closing the lower one after time Δt .

The sedimented particles were measured now in the scanning electron microscope from one angle of sight only, which saved much operation time.

2. Results

The times of sedimentation were always 26.6 seconds; the initial aerosol-free layers were 3.67, 2.66 and 0.33 mm, giving respectively minimal average velocity of sedimentation ($u_{i, min} \equiv \Delta s / \Delta t$) of 138 $\mu\text{m}/\text{sec}$, 100 $\mu\text{m}/\text{sec}$ and 12.4 $\mu\text{m}/\text{sec}$.

The dimensions of the particles found on the stubs under the conditions of those minimal settling velocities are given in Tables 6 through 8.

3. Analysis and discussion

Analyzing the results, one is still limited by the small number of particles determined. However, if one pools together particles of

$$l_i = l_{i,0} \pm \Delta l_i \quad \text{and} \quad c_i = c_{i,0} \pm \Delta c_i \quad \text{where} \quad \Delta l_i = 10 \mu m \quad \text{and}$$

$$\Delta c_i = 0.5 \mu m, \quad \text{then one obtains the Tables 9 through 11.}$$

l_i (μm)	c_i (μm)	l_i/c_i	l_i (μm)	c_i (μm)	l_i/c_i
71.5	2.54	28	21.9	0.49	45
18.0	0.33	55	86.1	0.97	89
11.9	0.87	14	59.4	1.67	36
15.8	1.71	9	35.1	4.58	8
12.1	0.31	39	26.7	0.66	41
80.2	1.71	47	18.3	0.34	54
29.4	1.01	29	47.3	0.34	138
42.3	1.46	29	36.3	2.78	13
80.7	2.89	28	16.5	0.37	45
4.7	0.58	8	58.9	1.59	37
6.7	1.45	5	9.4	2.17	4
13.4	0.42	32	97.2	10.62	9
18.3	0.36	51	26.8	0.87	31

../. .

ℓ_i (μm)	c_i (μm)	ℓ_i / c_i	ℓ_i (μm)	c_i (μm)	ℓ_i / c_i
8.8	0.52	17	44.5	1.35	33
55.8	1.33	42	30.2	1.43	21
27.0	1.52	18	18.9	0.76	25
28.0	0.83	34	14.0	1.13	12
78.7	1.72	46	7.74	0.99	8
57.5	1.84	31	99.6	1.04	96
81.0	1.53	53	60.9	1.17	52
26.1	0.82	32	45.9	0.80	57
46.8	0.77	61	42.9	0.91	47
70.5	0.73	97	29.9	2.92	10
7.4	0.93	8	40.9	2.19	19
6.1	0.9	7	27.4	0.75	36
8.9	1.13	8			

Table 6. The linear dimensions of cylindrical particles having
a settling velocity equal or greater than $138 \mu\text{m} / \text{sec}$.

l_i (μm)	c_i (μm)	l_i/c_i	l_i (μm)	c_i (μm)	l_i/c_i
16.2	0.64	25	21.3	2.29	9
22.3	1.30	17	28.7	1.45	20
52.9	1.14	46	11.7	1.96	6
52.1	1.25	42	10.8	1.46	49
143.1	0.83	172	34.6	2.74	13
47.8	1.14	42	72.9	1.05	69
64.2	1.40	46	49.1	1.36	36
38.9	0.81	48	50.3	1.14	44
54.1	1.18	46	12.7	1.00	13
40.0	1.01	40	25.3	2.18	12
62.3	1.36	46	36.8	0.94	39
41.6	1.36	32	88.8	1.75	51
65.4	1.18	55	48.8	1.67	29
95.2	1.58	60	47.9	1.43	34
31.0	2.52	12	66.8	2.41	28
19.6	0.85	23	9.4	2.40	4
21.2	1.25	17	75.8	0.39	194
130.9	2.25	62	20.1	1.94	10
68.6	0.90	76			

Table 7. The linear dimensions of cylindrical particles having a settling velocity equal or greater than $100 \mu m/sec$.

l_i (μm)	c_i (μm)	l_i/c_i	l_i (μm)	c_i (μm)	l_i/c_i
4.0	1.16	3	2.52	0.29	9
3.3	0.73	4	11.8	0.24	49
3.8	0.48	8	2.6	0.31	8
10.2	0.72	14	5.4	0.20	27
2.0	0.76	3	2.1	0.33	6
8.3	1.17	7	10.2	0.32	32
6.1	0.88	7	1.6	0.37	4
2.74	0.61	5	2.2	0.45	5
6.7	1.61	4	6.8	0.25	27
40.0	0.82	49	2.0	0.38	5
2.8	0.28	10	6.0	0.29	21
5.3	1.09	5	11.8	0.52	23
7.2	1.32	5	8.3	0.22	39
2.3	0.38	6	4.4	0.21	21
3.6	0.11	33	56.7	0.89	64
16.5	0.25	66	9.8	0.45	22
55.2	1.54	36	9.1	0.25	36
6.6	0.40	17	3.2	0.35	9
66.7	2.04	33	6.7	1.53	4
68.4	1.21	57	4.3	0.20	22
26.2	1.17	22	1.4	0.16	9
4.6	0.25	19	3.2	0.55	6
34.7	1.23	28	2.9	0.23	13
66.1	2.00	33	30.0	1.25	24
125.4	1.58	79	5.3	0.70	8
3.3	0.33	32	4.1	0.18	23
131.2	0.77	170	4.1	0.39	11
10.5	0.59	18			
7.8	0.29	27			
1.77	0.68	3			

Table 8. The linear dimensions of cylindrical particles having a settling velocity equal or greater than $12.4 \mu m/sec$.

$\ell_{i,o}(\mu m) \backslash c_{i,o}(\mu m)$	10	30	50	70	90
0.5	13	6	4	1	1
1.0	5	3	6	4	1

Table 9. η_{ℓ_i, c_i} for various values of $\ell_{i,o}$ and $c_{i,o}$.

$u_i \geq 138 \mu m/sec.$

$\ell_{i,o}(\mu m) \backslash c_{i,o}(\mu m)$	10	30	50	70
0.5	43	1	1	0
1.5	5	3	1	3

Table 10. η_{ℓ_i, c_i} for various values of $\ell_{i,o}$ and $c_{i,o}$.

$u_i \geq 100 \mu m/sec.$

$\ell_{i,o}(\mu m) \backslash c_{i,o}(\mu m)$	10	30	50	70
0.5	41	1	1	0
1.5	8	3	1	3

Table 11. η_{ℓ_i, c_i} for various values of $\ell_{i,o}$ and $c_{i,o}$.

$u_i \geq 12.4 \mu m/sec.$

According to the last three tables, Eq. [40], and the theoretical calculations of Gallily and Cohen (1976) for the probability appearing in Eqs. [40]-[41], one gets the final tables:

$\ell_{i,0}(\mu m) \backslash c_{i,0}(\mu m)$	10	30	50	70
0.5		55637	6452	775
1.5	339	138	461	34

Table 12. MLN_{ℓ_i, c_i} for various values of $\ell_{i,0}$ and $c_{i,0}$.
 $u_i \geq 138 \mu m/sec.$

$\ell_{i,0}(\mu m) \backslash c_{i,0}(\mu m)$	10	30	50	70
0.5		1387	621	0
1.5	315	122	35	96

Table 13. MLN_{ℓ_i, c_i} for various values of $\ell_{i,0}$ and $c_{i,0}$.
 $u_i \geq 100 \mu m/sec.$

$\ell_{i,0}(\mu m) \backslash c_{i,0}(\mu m)$	10	30	50	70
0.5	17320	298	252	0
1.5	452	116	33	93

Table 14. MLN_{ℓ_i, c_i} for various values of $\ell_{i,0}$ and $c_{i,0}$.
 $u_i \geq 12.4 \mu m/sec.$

As stated above, the frequency function f_{ℓ_i, c_i} can be now calculated from the values of $M L N_{\ell_i, c_i}$.

It should be remarked that the theoretical calculations of $P_{\ell_i, c_i, u_i, \Delta t}$ were based on continuous fluid values of the resistance coefficients.

Thus, for the case of Tables 12 and 13, no particles within the dimension-range of $\ell_i = 10 \pm 10 \mu m$ and $c_i = 0.5 \pm 0.5 \mu m$ could settle down on our stub in $\Delta t = 26.6$ sec. However, one should remember that for this range of sizes the resistance coefficients are smaller than the continuous medium ones and so this should have to be taken into account.

Judging from our rough results, it seems that the bi-parametric size distribution function f_{ℓ_i, c_i} of the glass fiber aerosol has a pronounced maximum at $\ell_{i,0} = 10 \mu m$ and $c_{i,0} = 0.5 \mu m$, and that it slopes down towards larger ℓ_i and c_i .

IV. T H E O R E T I C A L

Spatial distribution of sedimented cylindrical particles

The spatial distribution of sedimented cylindrical particles on an horizontal plane was calculated by a continuation of the theoretical study of Gallily and Cohen (Gallily, 1975; Gallily and Cohen, 1976).

Here, however, were used as systems of coordinates:

An internal cartesian system whose axes are parallel to the symmetry axes of the cylinder; a minor external cartesian system in which one axis is parallel to the direction of gravity, the other lies in a plane determined by the direction of gravity and the polar axis of the particle, and the third is perpendicular to the first two; a major external system based on the horizontal collecting surface and in which one axis is parallel to the direction of gravity.

1. Results

Typical results are given in Figs. 15 through 18.

The calculations were performed for:

- a. Continuous fluid resistance coefficients;
- b. Continuous fluid resistance coefficients corrected to account for the blunt edge by the multiplier $1.5^{1/3}$;
- c. Our regressed coefficients in an atmospheric pressure;
- d. Slip-flow coefficients, given by

$$K_{11} = K_{11,c} / (1 + \bar{\lambda}/\ell) \quad [42]$$

and

$$K_{33} = K_{33,c} / (1 + \bar{\lambda}/c) \quad [43]$$

where $\bar{\lambda}$, the mean free path of the air molecules, was taken to be $0.0653 \mu\text{m}$.

Observing Figs. [15] through [18], one should note that the sedimenting particle do have an overall drift, as found in an earlier study (Gallily, 1974), and that this drift decreases with increasing fall distance.

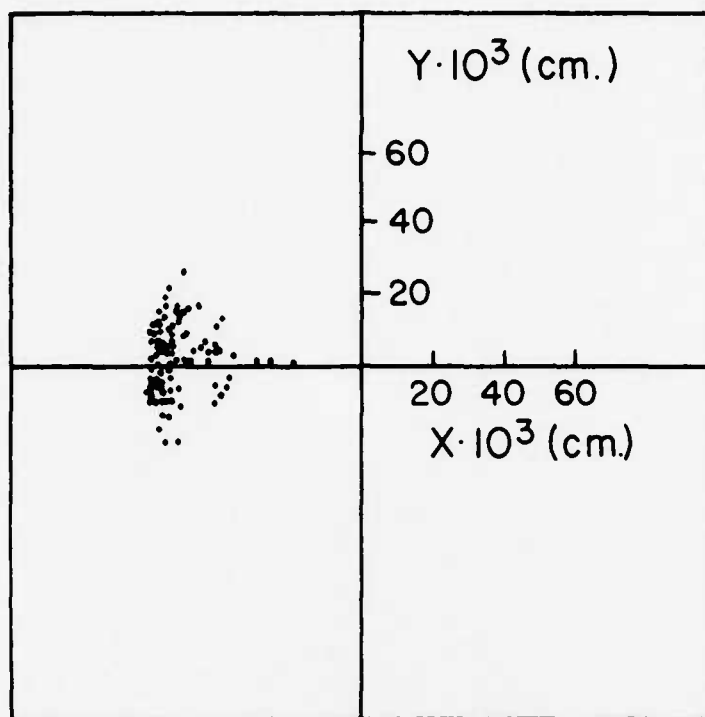


Fig. 15. Sedimentation points on an horizontal plane of cylinders of $12.3 \mu\text{m}$ length and $0.88 \mu\text{m}$ diameter which undergo a rotational brownian motion. Fall distance - 3.15 mm . Calculations parameter: Cylinders' density - 2.23 g.cm^{-3} , gravitational acceleration - $981 \text{ g.cm.sec}^{-2}$, air viscosity - $1.8 \cdot 10^{-4} \text{ c.g.s.}$, air temperature - 300°K , orientation change time - 10^{-1} sec ; Number of cylinders - 100, $\theta_{\text{initial}} = \pi/4$, azimuth angle_{initial} = 0. Average aerodynamic radius - $1.52 \mu\text{m}$, standard deviation of aerodynamic radii - $0.05 \mu\text{m}$. Translational resistance coefficients are continuous fluid values.

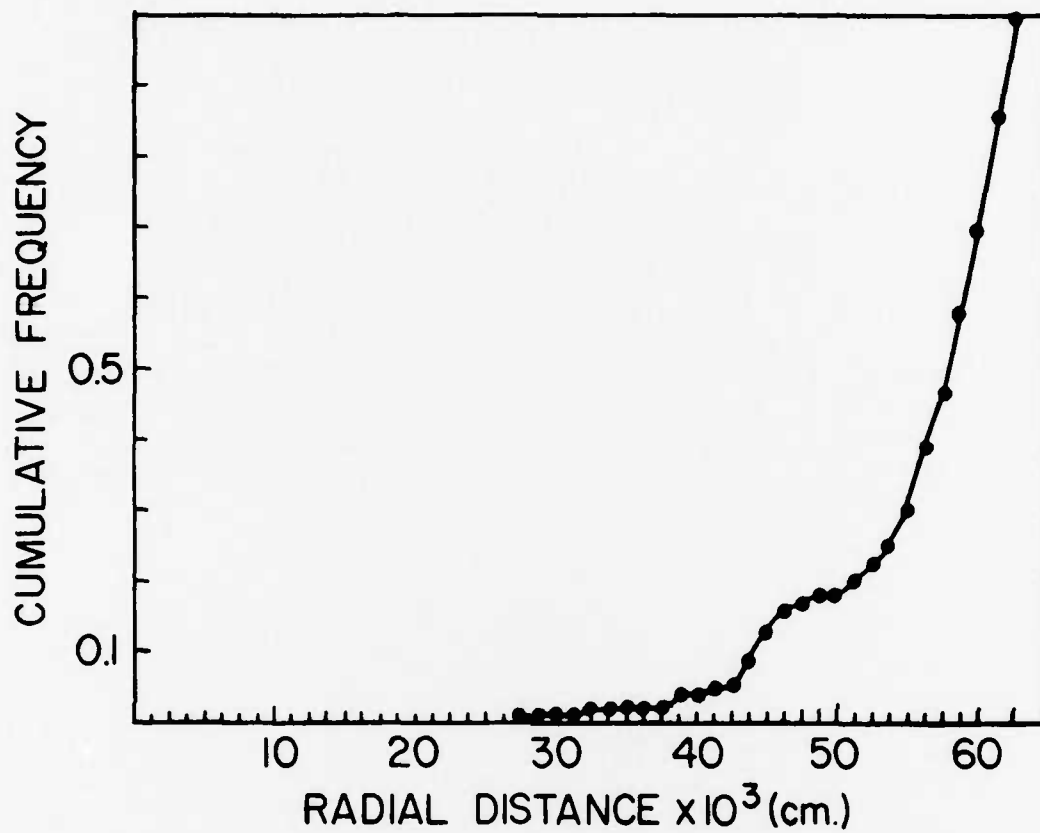


Fig. 16. Cumulative distribution of sedimented cylindrical particles vs. the radial distance from the origin of the main external coordinate system.

Same parameters of particles and calculations as given in legend to Fig. 15.

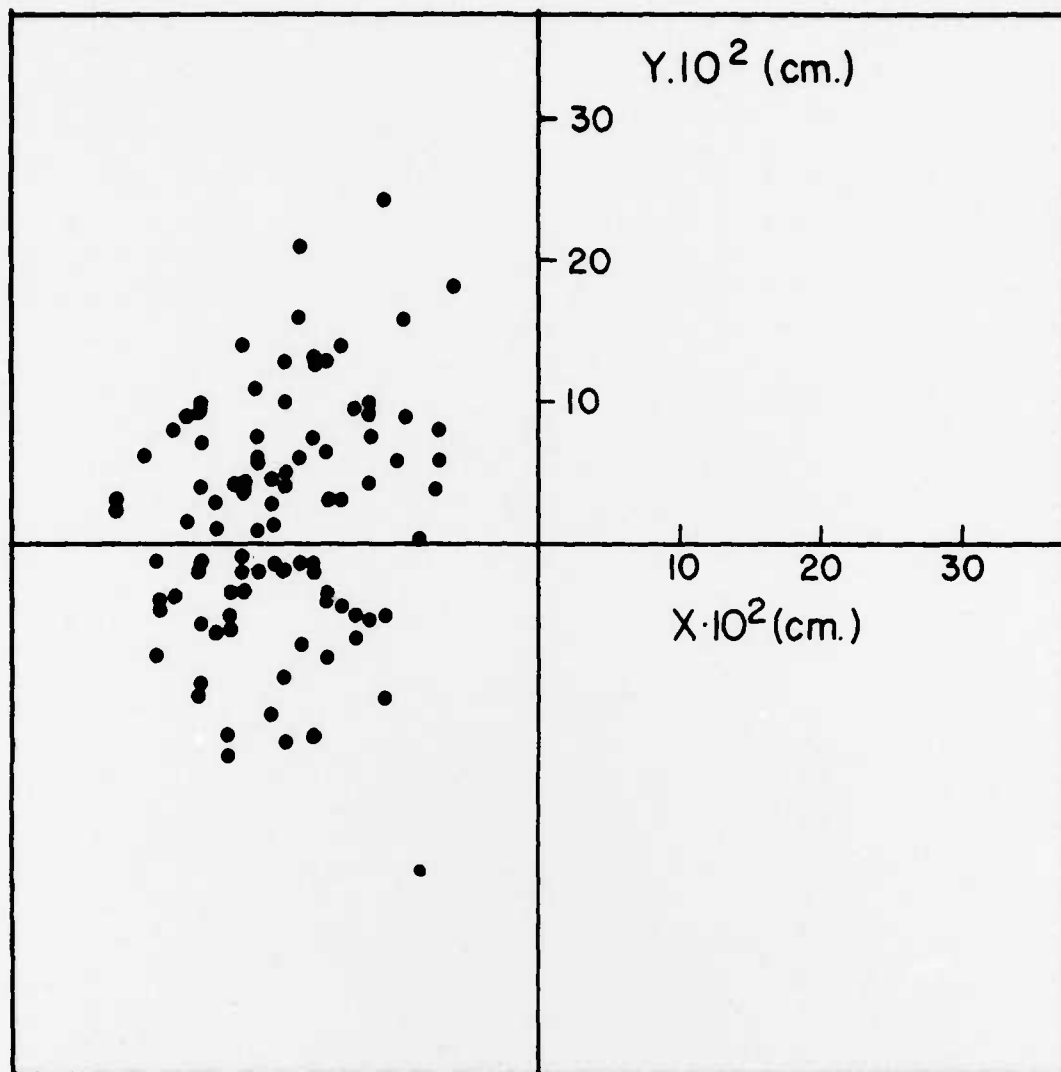


Fig. 17. Sedimentation points on an horizontal plane of cylinders of $13.1 \mu\text{m}$ length and $0.77 \mu\text{m}$ diameter which undergo a rotational Brownian motion. Fall distance - 16.55 mm. Calculation parameters: same as given in legend to Fig. 15. Average aerodynamic radius - $1.37 \mu\text{m}$; standard deviation of aerodynamic radii - 0.07μ .

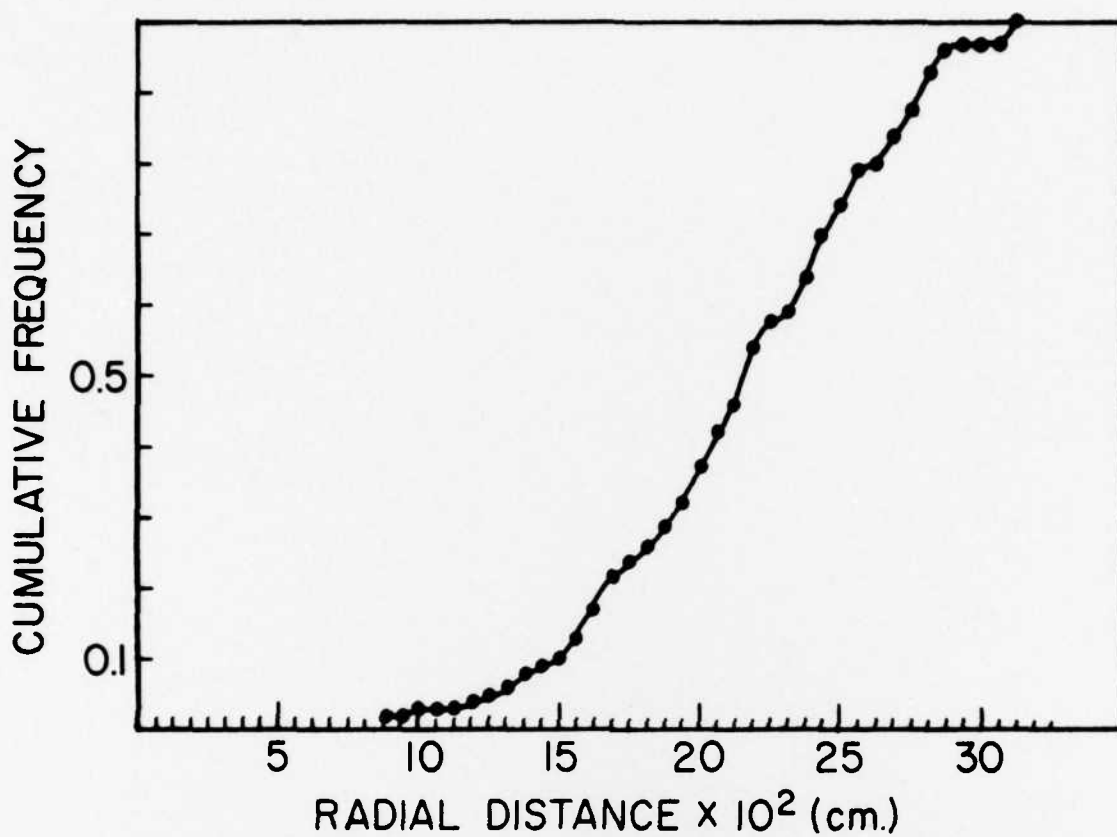


Fig. 18. Cumulative distribution of sedimented cylindrical particles vs. radial distance from the origin of the main external coordinate system.

Same parameters of particles as given in legend to Fig. 17;
same calculational parameters as given in legend to Fig. 15.

V. G L O S S A R Y

a, b, c - ellipsoidal particle's semi-axes

a - radius of a spherical particle

$A_1 - A_5$ - constants, defined in text

B - aerodynamic mobility of a particle;

\underline{B} - mobility tensor

c - diameter of a cylindrical particle

c_1 - number concentration of aerosol particles

C_m - factor, defined in text

d_s - diameter of a volumetrically equivalent particle; -

d_m - cross section diameter, defined in text

D_r - rotational diffusion coefficient of an axially symmetric particle about an equatorial axis

D^2, \square - operators, defined in text

D/Dt - the substantial derivative operator

f - fraction of gas molecules diffusely reflected from particle's surface with a temperature accommodation coefficient of 1.

$f_{(i,c)}$ - frequency function in size distribution of cylindrical particles.

\underline{F} - force acting on a particle; \underline{F}_e - external force; \underline{F}_f - fluiddynamic force

\underline{g} - gravitational acceleration

G - factor, defined in text

$\underline{i}, \underline{j}, \underline{k}$ - unit vectors along particles' principal translation axes

- k - Boltzmann's constant
- k_1 - coefficient related to cubical particles, defined in text
- K_n - Knudsen's number, defined in text; K_n' - Knudsen's number, defined in text
- $\underline{\underline{K}}$ - translation tensor; K_{ij} - components of tensor along translation principal axes (- coefficients of translational resistance);
- K - coefficient of cubical particles
- l - length of a cylindrical particle
- L - area of an observed field of view
- L_c - typical length of a particle
- $\underline{\underline{L}}_M$ - torque acting on the particle with respect to its center of mass M ; $\underline{\underline{L}}_{M,e}$ - external torque; $\underline{\underline{L}}_{M,f}$ - fluiddynamic torque
- m - mass of an aerosol particle
- m' - mass of fluid displaced by a particle
- M - number of field of views checked in size distribution analysis
- n_{r_i} - number of sedimented spherical particles of radius r_i which are counted
- N_{r_i} - number density of spherical aerosol particles
- n_{l_i,c_i} - number of sedimented cylindrical aerosol particles which are counted
- N_{l_i,c_i} - number density of cylindrical aerosol particles
- p - total pressure in gaseous medium
- $\underline{\underline{P}}$ - stress triadic defining $\underline{\underline{B}}$

$P_m(X)$ - Legendre's polynomial of degree

$P_{\ell_i, c_i, u_{\ell_i, c_i}, \Delta t}$ - probability of a cylindrical aerosol to have with the time Δt an average settling velocity u_{ℓ_i, c_i} , normalized so that $\sum_{u_i = \Delta s / \Delta t}^{u_i = u_{max}} P_{\ell_i, c_i} = 1$

Q - particle's intrinsic diadic, defined in text

\vec{r}_m - radius vector from center of mass to a surface point

R - radius of adjusted sphere

Re_t - translational Reynolds number, defined in text; Re_r - rotational number, defined in text

R_s - particle's Stokes radius; R_a - particle's aerodynamic radius

dS - surface element of a particle

S - surface of a particle

Δs - thickness of aerosol - free layer

t_1 - dummy variable

t - time; Δt - time difference

T - temperature (absolute scale), T_s - surface temperature

\vec{u}_m - translational velocity of particle's center of mass; \vec{u}_∞ - terminal sedimentation velocity ($u_{\infty, x}, u_{\infty, y}, u_{\infty, z}$ - components of velocity along external axes); $u_{\ell_i, c_i} (\equiv u_i)$ - sedimentation velocity of a cylindrical particle

\vec{v} - fluid velocity

x', y', z' - cartesian coordinates along particle's translational axes;

x, y, z - external coordinates (z - parallel to direction of gravity)

- $X = \cos \theta$ (θ - colatitude angle between the polar axis of an axially symmetric particle and an initial direction in space)
- Z - length of cube's side (Z_1, Z_2, Z_3 - three sides meeting in a corner); \bar{Z} - average value.

Greek Letters

- α, β, γ - integrals, defined in text
- α', β', γ' - direction cosines with respect to particle's translation
- Δ - defined in text
- λ - dummy variable
- $\bar{\lambda}$ - mean free path of gaseous molecules
- μ - dynamic viscosity of fluid
- ν - kinematic viscosity of the fluid
- χ_0 - integral, defined in text
- $\bar{\Pi}$ - stress tensor within a fluid
- ρ_p - density of a particle
- ζ_t - tangential stress on particle's surface
- $\phi = 1/c$
- ψ - sphericity factor
- ω - rotational velocity of the particle

Subscripts

- c - continuous regime value
- e - external
- F - fluiddynamic
- i - i-th
- M - center of mass
- o - central value
- t - tangential

VI. LITERATURE CITED.

- Brenner, H., 1961: Chem. Engrg.Sci. 16, 242.
- , 1964: The Stokes resistance of an arbitrary particle - IV. Arbitrary field of flow, Chem. Engrg. Sci. 19, 703.
- , (in Happel J. and Brenner, H.) 1965a: Low Reynolds Number Hydrodynamics, Prentice-Hall, N.J, pp. 205, 225.
- , 1965b: *ibid*, p. 231.
- , Goldman, A.J. and Cox, R.G, 1967: Slow viscous motion of a sphere parallel to a plane wall - II. Couette flow, Chem. Engrg. Sci. 22, 653.
- , and Condiff D.W., 1972: Transport mechanics in systems of orientable particles, J. Colloid Interface Sci. 41, 228.
- Dahneke, B.E., 1973a: Slip correction factor for nonspherical bodies, II. Free molecule flow, J. Aerosol.Sci. 4, 147.
- , 1973b: Slip correction factor for nonspherical bodies. II. The form of the general law, *ibid*. p. 163.
- De Mestre, N.J. and Russel, W.B., 1975: Low-Reynolds number translation of a slender cylinder near a plane wall, J. Engrg. Mat. 2, 81.
- Epstein, P.S., 1924: Phys.Rev. 23, 710.
- Gallily, Isaiah, 1969: Technical Innovations, Jet Propulsion Laboratory, California Institute of Technology, Pasadena, California.

Gallily, Isaiah and Mahrer, Y., 1973: On the motion of a spherical aerosol particle near a wall, Aerosol Sci. 4, 253.

—————, 1974: The Dynamics of Nonspherical Aerosol Particles. I. Controlled Generation of Nonspherical Aerosols and Methods for their size, Concentration and Electric Charge Measurement, Final Technical Report, European Research Office, U.S. Army, Contract DAJA37-72-3878, p.1.

—————, 1975: The Dynamics of Nonspherical particles. II. Mobility in non-orienting Fields, Final Technical Report, European Research Office, U.S. Army, Contract DAJA37-74-C-1208, p.74.

—————, and Cohen, A.H., 1976: On the stochastic nature of the motion of nonspherical aerosol particles. I. The aerodynamic radius concept, J. Colloid and Interface Sci. 56, 443.

—————, 1977: The Dynamics of Nonspherical Particles. III. Mobility and Deposition in Still Air, present Final Technical Report.

Gans, R., 1928: Zur Theorie der Brownschen Molekularbewegung, Annalen der Phys. 86, 628.

Gentry, J. and Spurny, K., 1976: The effect of orientation on the optical and collection properties of fibers, GAF Congress, 1976, Bad-Soden, Germany.

Happel J. and Brenner, H., 1965a: Low Reynolds Number Hydrodynamics, Prentice-Hall, N.J.. p. 164.

————— and —————, 1965b: *ibid*, p. 225.

- Heiss, J.F. and Coull, J., 1952: The effect of orientation and shape on the settling velocity of nonisometric particles, Chem. Engrg. Prog., 48, 133.
- Hochrainer D. and Hänel, G., 1975: Der dynamische Formfactor nicht-kugelförmiger Teilchen als Funktion des Luftdrucks, J. Aerosol Sci. 6, 97.
- Horvath, H., 1974: Das Fallverhalten nicht-kugelförmiger Teilchen, Staub, 34, 251.
- Jayaweera, K.O.L.F and Curtis, R.E., 1969: Fall velocities of plate-like and columnar-like ice crystals, Quart. J. Roy. Met. Soc. 95, 703.
- Kajkawa, M., 1971: A model experimental study on the falling velocity of ice crystals, J. Met. Soc. Japan 49, 367.
- Kotrappa, P., 1972: Shape factors for aerosols of coal, UO_2 , and ThO_2 in respirable size range, in "Assessment of Airborne Particles (Merar, Morrow and Stöber, eds.) Thomas, Chap. 16.
- Lamb, H., 1932: Hydrodynamics, Dover, New York, pp. 152-5.
- Morrison, F.A., 1974a: Inertial impaction in stagnation flow, J. Aerosol Sci. 5, 241.
- Morrison, F.A. and Reed, L.D., 1974b: Particle interactions in viscous flow at small values of Knudsen Number, J. Aerosol Sci, 5, 175.
- Pettyjohn, E.S. and Christiansen, E.B., 1948: Effect of particle shape on free-settling rates of isometric particles Chem. Engrg. Prog. 44, 157.

Pich, J., 1967: The drag of a cylinder in the transition region, J. Colloid Interface, sci., 29, 91.

Stern, A.C. (ed), 1968: Air Pollution (Second Edition), Academic Press, New York, p. 72.

Stöber, W., 1972: Dynamic shape factors of nonspherical aerosol particles, in Assessment of Airborne Particles (Mercer, Morrow and Stöber, eds), Thomas, Chap 14.

———, 1975: Private communication.

Schwartz, M.H. and Andres, R.P., 1976: Theoretical basis of the time-of-flight aerosol spectrometer, J. Aerosol Sci., 7, 281.

Wakiya, S., 1959: Effect of a submerged object on a slow viscous flow (Report V). Spheroid at an arbitrary angle of attack No. 8 Res. Rep. Fac. Eng. Niigata Univ. (Japan).

Walkenhorst, W., 1976: Modellversuche zur Bestimmung des dynamischen Formfaktors nicht isometrischer Teilchen, Staub, 36, A 149.

This study has been carried out by Prof. Isaiah Gallily,
Mr. M. Weiss (M.Sc), Mr. A. H. Cohen (M.Sc.), and Mr. B. Kerner
as a technical assistant.

ATE
LMED
-7